Non-linear Dynamics in Queueing Theory: Determining Size of Oscillations in Queues with Delayed Information

Sophia Novitzky
Center for Applied Mathematics
Cornell University
657 Rhodes Hall, Ithaca, NY 14853
sn574@cornell.edu

Jamol Pender
School of Operations Research and Information Engineering
Cornell University
228 Rhodes Hall, Ithaca, NY 14853
jjp274@cornell.edu

Richard H. Rand
Sibley School of Mechanical and Aerospace Engineering
Department of Mathematics
Cornell University
535 Malott Hall, Ithaca, NY 14853
rand@math.cornell.edu

Elizabeth Wesson
Center for Applied Mathematics
Cornell University
Rhodes Hall 657, Ithaca, NY 14853
enw27@cornell.edu

October 10, 2018

Abstract

With the advancement of online technologies, services often provide waiting time or queue length information to customers. This information allows the customers to determine whether to remain in line or in the case of multiple lines, which line to join. Unfortunately, there is usually a delay associated with the waiting time information: either the information is not provided in real time or it takes the customers travel

time to join the service after having received the information. Recent empirical and theoretical work uses functional dynamical systems as models for queueing systems and shows that if information is delayed long enough, a Hopf bifurcation can occur and cause unwanted oscillations in the queues. However, it is not known how large the oscillations are when a Hopf bifurcation occurs. To answer this question, we model queues with functional differential equations and implement two methods for approximating the amplitude of the oscillations. The first approximation is analytic and yields a closed-form approximation in terms of the model parameters. The second approximation uses a statistical technique, and delivers highly accurate approximations over a wider parameter range than does the first method.

Keywords: Hopf bifurcation, delay-differential equation, perturbations method, Lindstedt's method, operations research, queueing theory

AMS subject classifications: 34K99, 35Q94, 41A10, 37G15

1 Introduction

The omnipresence of smartphone and internet technologies has created new ways for corporations and service system managers to interact with their customers. One important and common example of such communication is the delay announcement, which has become the main tool for service system managers to inform customers of their estimated waiting time. Currently, delay announcements are ubiquitous in most call centers and telecommunications networks and are vital to the customer experience. Another example exists in healthcare where many hospitals now display their wait times online as a way of enticing patients to come to their hospital for treatment. Another application where customers receive information about the system is in the context of transportation, where highway display message signs (DMS) display information about the traffic ahead as a way to direct and mitigate highway congestion.

The reason why delay announcements are so popular among service providers is that they can influence the decisions of customers as well as the queue length dynamics of the system as seen in [1]. As a result, delay announcements are of major interest among researchers who aim to quantify the impact of delay announcements on the queue length process or the virtual waiting time process. The work of [2, 3, 4, 5, 6, 7, 8, 9, 10, 11] and references therein focus on this aspect of the announcements.

The analysis of this paper is similar to the main thrust of the delay announcement literature in that it is concerned with the impact of the information on the dynamics of the queueing process. However, the current literature focuses only on services that give the delay announcements to their customer in real-time, while we consider the scenarios when the information itself is delayed. Our analysis also applies to systems where the information is given in real-time, but the customer may need time to travel to receive their service. This scenario occurs quite often in transportation settings.

This delay in information is commonly experienced in services that use smartphone apps or websites to inform their customers about about the waiting times prior to customers' arrival to the service. One example is the Citibike bike-sharing network in New York City

([12, 13]). Riders can search the availability of bikes on a smartphone app. However, in the time that it takes for them to leave their home and get to a station, all of the bikes could have been taken. Thus, the information that they used was in real-time, but their travel time makes it delayed and somewhat unreliable as the system can change before they arrive. The same situation occurs in amusement parks like Disneyland or Six Flags that list waiting times and the rider's current distance from each ride in the theme park. Finally, the emergency rooms of near-by hospitals face the same issue when they display their waiting times online as it takes the patients some time to reach the emergency room.

However, one major difference of our work from the current literature is that we use functional differential equations to model the queue length processes. Typically, it is common to use ordinary differential equations to model the mean dynamics of the queue length processes, but here we model the delayed information via delay differential equations and functional differential equations with moving averages. As a result, the analysis is quite complicated since many functional differential equations are infinite dimensional and are much more nuanced than their ordinary differential equation counterparts. The work [14] uses delay differential equations within the context of sizing router buffers in the Internet, proving the this approach to be useful. The mathematical model in [14] is quite different than the one in this paper, however. Also, the recent work by [15] explores the use of delay differential equations in the context of queueing models with delayed information, but they neglect essential quantities of interest. Although [15] explores when a Hopf bifurcation will occur, they do not analyze how large and how often oscillations will occur in the queueing models. A rigorous understanding of the size of oscillations is critical to making informed decisions about queues with delayed information and our work in this paper addresses this very important problem.

1.1 Paper Outline

This paper considers two models of queues that were originally presented in [15] and [16] as fluid limits of stochastic queueing models. In each model, there are two queues and the customers decide which queue to join based on information about the queue length that is in some way delayed by a constant parameter Δ. We analyze the qualitative behavior in both cases, stating the conditions for a unique stable equilibrium, as well as the conditions for supercritical Hopf bifurcations. We focus on the behavior of the queues when the stable equilibrium first transitions into a stable limit cycle, and approximate the amplitude of the resulting oscillations. At first, we use Lindstedt's method, a modified perturbation method, which is accurate on a limited range of the parameters. To broaden this range, we implement a statistical method that uses known amplitude of a small subset of queues and extrapolates it for a larger set of parameters. Overall, this method obtains higher accuracy when compared to Lindstedt's method for larger values of the delay. These approximations are important as the amplitude of queue oscillations can provide important insights such as the average waiting time during the busier hours, the longest waiting time a customer can experience, and the optimal moment of joining the queue that will guarantee the quickest service.

2 Constant Delay Model

In a model with two infinite-server queues visualized by Figure (1), customers arrive at a rate $\lambda > 0$. Each customer is given a choice of joining the first or the second queue. The customer is told about the queue lengths, and is likely to prefer the shorter queue. The probability of joining a given queue is given by the Multinomial Logit Model (MNL)

$$p_i(q(t), \Delta) = \frac{\exp(-q_i(t-\Delta))}{\exp(-q_1(t-\Delta)) + \exp(-q_2(t-\Delta))} \tag{2.1}$$

where p_i is the probability of i^{th} queue being joined, and $q_i(t)$ is the length of i^{th} queue at time t. The MNL is very commonly used to model customer choice in fields of operations research, economics, and applied psychology ([17, 18, 19, 20]). The delay $\Delta > 0$ can be interpreted as either the customers' travel time to the service or the time lag between when the queue length measurement is taken and when the information is posted for the customers to see. The model assumes an infinite-server queue, which is customary in operations research literature ([21, 22, 23]). This assumption implies that the departure rate for a queue is the service rate $\mu > 0$ multiplied by the total number of customers in that queue. Therefore the queue lengths can be described by

$$\dot{q}_1(t) = \lambda \cdot \frac{\exp(-q_1(t-\Delta))}{\exp(-q_1(t-\Delta)) + \exp(-q_2(t-\Delta))} - \mu q_1(t) \tag{2.2}$$

$$\dot{q}_2(t) = \lambda \cdot \frac{\exp(-q_2(t-\Delta))}{\exp(-q_1(t-\Delta)) + \exp(-q_2(t-\Delta))} - \mu q_2(t) \tag{2.3}$$

for $t > 0$, with initial conditions specified by nonnegative continuous functions f_1 and f_2

$$q_1(t) = f_1(t), \quad q_2(t) = f_2(t), \quad t \in [-\Delta, 0]. \tag{2.4}$$

The following Section describes the qualitative behavior of the queues (2.2) - (2.3) and the influence of the parameters λ, μ, and Δ on the system.

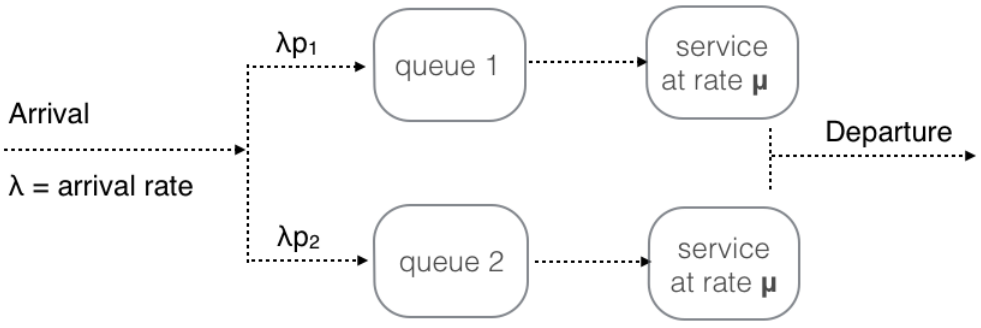

Figure 1: Customers going through a two-queue service system.

2.1 Hopf Bifurcations in the Constant Delay Model

The system of equations (2.2) - (2.3) can be uncoupled when the sum and the difference of q_i is taken. The system is reduced to the equations

$$\dot{v}_1(t) = \dot{q}_1(t) - \dot{q}_2(t) = \lambda \tanh\left(\frac{1}{2}v_1(t-\Delta)\right) - \mu v_1(t), \tag{2.5}$$

$$\dot{v}_2(t) = \dot{q}_1(t) + \dot{q}_2(t) = \lambda - \mu v_2(t), \tag{2.6}$$

where $v_2(t)$ is solvable, and the equation on $v_1(t)$ is of a form commonly studied in the literature. Many papers (such as [24, 25, 26, 27, 28]) prove properties about the limit cycles for models similar to ours. The frequency of oscillations for a similar model is studied in [29]. In [26], the author uses asymptotic analysis to prove uniqueness and stability of the slowly oscillating periodic solutions that occur under certain parameter restrictions. Our paper complements these results by developing an approximation for the amplitude of the oscillations near the first bifurcation point.

When the delay is sufficiently small, the queues converge to the stable equilibrium

$$q_1^*(t) = q_2^*(t) = \frac{\lambda}{N\mu}, \tag{2.7}$$

where N is the number of queues. The existence and uniqueness of the equilibrium is shown in Theorem (2.3). The stability is given by Theorem (2.4). The equilibrium is stable, in part, because all pairs of complex eigenvalues shift to the negative real half of the complex plane as the delay approaches zero, by Proposition (2.8).

As the delay increases, however, infinitely many pairs of complex eigenvalues may cross the imaginary axis. When the first pair of complex eigenvalues crosses, the queues undergo a supercritical Hopf bifurcation, and the stable equilibrium point turns into a stable limit cycle. Figures (2) - (3) show this transition in behavior. The delay at which this bifurcation occurs is given by the smallest nonnegative root of Equation (2.15). However, every subsequent pair of eigenvalues crossing will result in a supercritical Hopf bifurcation as well. Theorem (2.1) shows the existence of these Hopf bifurcations, and Theorem (2.2) proves their stability.

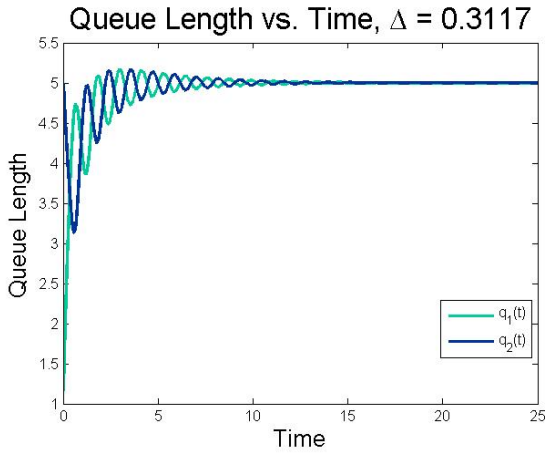

Figure 2: $\lambda = 10$, $\mu = 1$, $\Delta < \Delta_{cr}$.

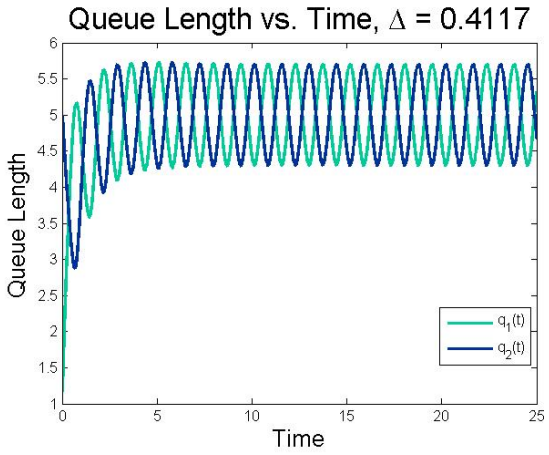

Figure 3: $\lambda = 10$, $\mu = 1$, $\Delta > \Delta_{cr}$.

To determine the threshold Δ_{cr} at which a bifurcation may occur, we first introduce the functions $\tilde{u}_i(t)$ that represent the deviation of q_i from the equilibrium:

$$\tilde{u}_i(t) = q_i(t) - q_i^* = q_i(t) - \frac{\lambda}{N\mu}. \tag{2.8}$$

It is sufficient to analyze the stability of the linearized system of equations in order to determine the stability of $q_i(t)$ ([30], [31]). Hence we will consider

$$\dot{\tilde{u}}_1(t) \approx -\frac{\lambda}{4}\Big(\tilde{u}_1(t-\Delta) - \tilde{u}_2(t-\Delta)\Big) - \mu\tilde{u}_1(t) \tag{2.9}$$

$$\dot{\tilde{u}}_2(t) \approx -\frac{\lambda}{4}\Big(\tilde{u}_2(t-\Delta) - \tilde{u}_1(t-\Delta)\Big) - \mu\tilde{u}_2(t). \tag{2.10}$$

Equations (2.9)-(2.10) can be uncoupled by the following transformation

$$\tilde{v}_1(t) = \tilde{u}_1(t) + \tilde{u}_2(t), \quad \tilde{v}_2(t) = \tilde{u}_1(t) - \tilde{u}_2(t), \tag{2.11}$$

$$\dot{\tilde{v}}_1(t) = -\mu\left(\tilde{u}_1(t) + \tilde{u}_2(t)\right) = -\mu\tilde{v}_1(t), \tag{2.12}$$

$$\dot{\tilde{v}}_2(t) = -\frac{\lambda}{2}\cdot\tilde{v}_2(t-\Delta) - \mu\tilde{v}_2(t). \tag{2.13}$$

While $\tilde{v}_1(t)$ decays exponentially to 0, $\tilde{v}_2(t)$ undergoes a Hopf bifurcation at Δ_{cr}, which we intend to show. Assuming the solution of the form $\tilde{v}_2(t) = \exp(\Lambda t)$, the characteristic equation for $\tilde{v}_2(t)$ becomes

$$\Phi(\Lambda, \Delta) = \Lambda + \frac{\lambda}{2}\exp(-\Lambda\Delta) + \mu = 0. \tag{2.14}$$

We assume $\Lambda = i\omega_{cr}$ with $\omega_{cr} > 0$, plug Λ into (2.14), separate the real and imaginary parts into two equations, and use the trigonometric identity $\cos^2(\omega\Delta) + \sin^2(\omega\Delta) = 1$ to find

$$\Delta_{cr}(\lambda, \mu) = \frac{2\arccos(-2\mu/\lambda)}{\sqrt{\lambda^2 - 4\mu^2}}, \quad \omega_{cr} = \sqrt{\frac{\lambda^2}{4} - \mu^2}. \tag{2.15}$$

For ω_{cr} to be real the condition $\frac{\lambda^2}{4} - \mu^2 > 0$ must hold, so $\lambda > 2\mu$. If this condition is met, the stable equilibrium is lost when Δ exceeds the **smallest nonnegative root** of Δ_{cr} from Equation (2.15). It is worthwhile to note, however, that a **Hopf bifurcation occurs at every root** of Δ_{cr}, as demonstrated in Theorem (2.1).

Theorem 2.1. *If $\lambda > 2\mu$, a Hopf bifurcation occurs at $\Delta = \Delta_{cr}$, where Δ_{cr} is given by*

$$\Delta_{cr}(\lambda, \mu) = \frac{2\arccos(-2\mu/\lambda)}{\sqrt{\lambda^2 - 4\mu^2}}. \tag{2.16}$$

Proof. When Δ is close to zero, all complex eigenvalues are on the real negative half of complex plane, and they pass the imaginary axis from left to right as Δ increases . One pair passes at each root of Δ_{cr}, and afterwards this pair remains in the positive half of the complex plain (Proposition (2.7)). At each root of Δ_{cr} there is one purely imaginary pair of

eigenvalues, but all other eigenvalues necessarily have a nonzero real part. Hence all roots $\Lambda_j \neq \Lambda^+, \Lambda^-$ satisfy $\Lambda_j \neq m\Lambda^+$ for any integer m.

By introducing $\Lambda = \alpha(\Delta) + i\omega(\Delta)$ into the characteristic equation (2.14), we show that Re $\Lambda'(\Delta_{cr}) \neq 0$ through implicit differentiation:

$$\frac{d\alpha}{d\Delta} = \frac{\lambda\Delta}{2}e^{-\alpha\Delta}\cos(\omega\Delta)\frac{d\alpha}{d\Delta} + \frac{\lambda\alpha}{2}e^{-\alpha\Delta}\cos(\omega\Delta) + \frac{\lambda\omega}{2}e^{-\alpha\Delta}\sin(\omega\Delta), \tag{2.17}$$

$$\frac{d\alpha}{d\Delta} = \Big(\frac{\lambda}{2}e^{-\alpha\Delta}\Big)\cdot\frac{\alpha\cos(\omega\Delta) + \omega\sin(\omega\Delta)}{1 - \frac{\lambda\Delta}{2}e^{-\alpha\Delta}\cos(\omega\Delta)}, \tag{2.18}$$

$$\frac{d\alpha(\Delta_{cr})}{d\Delta} = \Big(\frac{\lambda}{2}\Big)\cdot\frac{\omega_{cr}\cdot\frac{\omega_{cr}2}{\lambda}}{1 - \frac{\lambda\Delta}{2}\cdot\big(-\frac{2\mu}{\lambda}\big)} = \frac{\frac{\lambda^2}{4} - \mu^2}{1 + \mu\Delta_{cr}} \neq 0. \tag{2.19}$$

Hence, all conditions of the infinite-dimensional version of the Hopf theorem from [30] are satisfied, so a Hopf bifurcation occurs at every root Δ_{cr}. □

Theorem 2.2. *The Hopf bifurcations given by Theorem* (2.1) *are supercritical, i.e. each Hopf produces a stable limit cycle in its center manifold.*

Proof. We will use the method of *slow flow*, or the Method of Multiple Scales, to determine the stability of the Hopf bifurcations given by Theorem (2.1). This method is often applied to systems of delay differential equations (DDEs) [32, 33, 34].

The first step is to consider the perturbation of q_1 and q_2 from the equilibrium point $q_1^* = q_2^* = \frac{\lambda}{2\mu}$ given in Equation (2.7), and to approximate the resulting derivatives by third order Taylor expansion. This is done in Section 5.1.2. The resulting DDEs are

$$\dot{w}_1(t) = \lambda\Big(-\frac{w_1 - w_2}{4} + \frac{w_1^3 - 3w_2w_1^2 + 3w_1w_2^2 - w_2^3}{48}\Big)(t-\Delta) - \mu w_1(t) \tag{2.20}$$

$$\dot{w}_2(t) = \lambda\Big(-\frac{w_2 - w_1}{4} + \frac{w_2^3 - 3w_1w_2^2 + 3w_2w_1^2 - w_1^3}{48}\Big)(t-\Delta) - \mu w_2(t). \tag{2.21}$$

By considering the sum and the difference of w_1 and w_2, we can uncouple the two equations:

$$\dot{\tilde{v}}_1(t) = -\mu\tilde{v}_1(t) \tag{2.22}$$

$$\dot{\tilde{v}}_2(t) = \lambda\left(-\frac{\tilde{v}_2(t-\Delta)}{2} + \frac{\tilde{v}_2^3(t-\Delta)}{24}\right) - \mu\tilde{v}_2(t). \tag{2.23}$$

For details, see Section 5.1.3. The function $\tilde{v}_1(t) = Ce^{-\mu t}$ decays to 0, while the function $\tilde{v}_2(t)$ has a Hopf bifurcation at Δ_{cr} where the periodic solutions are born.

We set $\tilde{v}_2(t) = \sqrt{\epsilon}x(t)$ in order to prepare the DDE for perturbation treatment, giving

$$\dot{x}(t) = \lambda\left(-\frac{x(t-\Delta)}{2} + \frac{\epsilon x^3(t-\Delta)}{24}\right) - \mu x(t). \tag{2.24}$$

We replace the independent variable t by two new time variables $\xi = \omega t$ (stretched time) and $\eta = \epsilon t$ (slow time). Then we expand Δ and ω about the critical Hopf values:

$$\Delta = \Delta_{cr} + \epsilon\alpha, \quad \omega = \omega_{cr} + \epsilon\beta. \tag{2.25}$$

The time derivative $\dot{x}$ becomes

$$\dot{x} = \frac{dx}{dt} = \frac{\partial x}{\partial \xi}\frac{d\xi}{dt} + \frac{\partial x}{\partial \eta}\frac{d\eta}{dt} = \frac{\partial x}{\partial \xi} \cdot (\omega_{cr} + \epsilon\beta) + \frac{\partial x}{\partial \eta} \cdot \epsilon. \tag{2.26}$$

The expression for $x(t-\Delta)$ may be simplified by Taylor expansion for small ϵ:

$$\begin{aligned} x(t-\Delta) &= x(\xi - \omega\Delta, \eta - \epsilon\Delta) && (2.27)\\ &= x(\xi - (\omega_{cr} + \epsilon\beta)(\Delta_{cr} + \epsilon\alpha), \eta - \epsilon(\Delta_{cr} + \epsilon\alpha)) + O(\epsilon^2) && (2.28)\\ &= \tilde{x} - \epsilon(\omega_{cr}\alpha + \Delta_{cr}\beta) \cdot \frac{\partial \tilde{x}}{\partial \xi} - \epsilon\Delta_{cr}\frac{\partial \tilde{x}}{\partial \eta} + O(\epsilon^2), && (2.29) \end{aligned}$$

where $x(\xi - \omega_{cr}\Delta_{cr}, \eta) = \tilde{x}$. The function x is represented as $x = x_0 + \epsilon x_1 + \ldots$, and we get

$$\frac{dx}{dt} = \omega_{cr}\frac{\partial x_0}{\partial \xi} + \epsilon\beta\frac{\partial x_0}{\partial \xi} + \epsilon\frac{\partial x_0}{\partial \eta} + \epsilon\omega_{cr}\frac{\partial x_1}{\partial \xi}. \tag{2.30}$$

We substitute (2.29) and (2.30) into (2.24), and separate the terms of equal powers of ϵ

$$\omega_{cr}\frac{\partial x_0}{\partial \xi} + \frac{\lambda}{2}\tilde{x}_0 + \mu x_0 = 0, \tag{2.31}$$

$$\omega_{cr}\frac{\partial x_1}{\partial \xi} + \frac{\lambda}{2}\tilde{x}_1 + \mu x_1 = -\beta x_{0\xi} - x_{0\eta} + \frac{\lambda}{2}\big(\beta\Delta_{cr} + \alpha\omega_{cr}\big) \cdot \tilde{x}_{0\xi} + \frac{\lambda}{24}\tilde{x}_0^3. \tag{2.32}$$

Equation (2.31) shows that x_0 can be written as $x_0(t) = A(\eta)\cos(\xi) + B(\eta)\sin(\xi)$. Eliminating the secular terms $\sin(\xi)$ and $\cos(\xi)$, we get two equations that involve $\frac{d}{d\eta}A(\eta)$ and $\frac{d}{d\eta}B(\eta)$, and we get rid of the delay terms by using Equation (2.31). We introduce $R(\eta) = \sqrt{A(\eta)^2 + B(\eta)^2}$, and find $\frac{dR}{d\eta}$:

$$\frac{dR}{d\eta} = -\frac{R\Big((\Delta_{cr}\lambda^2 + 4\mu)R^2 - 16\alpha(\lambda^2 - 4\mu^2)\Big)}{16(4 + \Delta_{cr}^2\lambda^2 + 8\Delta_{cr}\mu)}. \tag{2.33}$$

Since $R \geq 0$ by definition, the two equilibrium points are

$$R_1 = 0, \quad R_2 = \sqrt{\frac{16\alpha(\lambda^2 - 4\mu^2)}{(\Delta_{cr}\lambda^2 + 4\mu)}}. \tag{2.34}$$

The stability of these equilibrium points follows directly from the direction of the flow (2.33) on the R-line. The equilibrium point R_1 is unstable and R_2 is stable. Thus the limit cycle born when Δ exceeds any root of Δ_{cr} is locally stable in its center manifold. □

Theorem 2.3. *For sufficiently small Δ, the unique equilibrium to the system of N equations*

$$\dot{q}_i(t) = \lambda \cdot \frac{\exp(-q_i(t-\Delta))}{\sum_{j=1}^{N}\exp(-q_j(t-\Delta))} - \mu q_i(t) \tag{2.35}$$

is given by

$$q_i^*(t) = \frac{\lambda}{N\mu} \quad \forall i = 1, 2, \cdots, N. \tag{2.36}$$

Proof. See the Appendix for the proof. □

Theorem 2.4. *The equilibrium point of Equations* (2.2) - (2.3) *is stable when* Δ *is less than the smallest nonnegative root of* Δ_{cr}.

Proof. Any real eigenvalue must be negative because the characteristic equation $\Phi(\Lambda, \Delta) = \Lambda + \frac{\lambda}{N}\exp(-\Lambda\Delta) + \mu > 0$ whenever $\Lambda \geq 0$, $\Lambda \in \mathbb{R}$. Now consider the complex eigenvalues. Proposition (2.8) states that for any complex eigenvalue Λ, $\mathrm{Re}[\Lambda] < 0$ when $\Delta \to 0^+$, and we have shown that $\mathrm{Re}[\Lambda] = 0$ only when $\Delta = \Delta_{cr}$. Also, Λ is continuous as a function of Δ, which implies that $\mathrm{Re}[\Lambda] < 0$ for all Δ less than the smallest positive root Δ_{cr} from (2.15). Therefore when Δ is in the specified range, all eigenvalues have negative real parts so the equilibrium must be stable. □

Proposition 2.5. *If there is a root* $r = x + iy$ *of the characteristic equation*

$$r = \alpha + \beta e^{-r\Delta} \tag{2.37}$$

with positive real part ($x > 0$) *then it is bounded by* $x \leq \alpha + |\beta|$ *and* $|y| \leq |\beta|$.

Proof. Plug $r = x + iy$ into Equation (2.37) and separate real and imaginary parts to get

$$\cos(y\Delta) = \frac{e^{x\Delta}(x - \alpha)}{\beta}, \quad \sin(y\Delta) = -\frac{e^{x\Delta}y}{\beta} \tag{2.38}$$

These equations give the inequalities

$$-1 \leq \frac{e^{x\Delta}(x - \alpha)}{\beta} \leq 1, \quad -1 \leq -\frac{e^{x\Delta}y}{\beta} \leq 1 \tag{2.39}$$

Assuming that $x > 0$ and $\Delta \geq 0$, we know that $e^{x\Delta} \geq 1$. Therefore inequalities reduce to

$$-1 \leq \frac{(x - \alpha)}{\beta} \leq 1, \quad -1 \leq -\frac{y}{\beta} \leq 1, \tag{2.40}$$

and give the desired bounds $x \leq \alpha + |\beta|$ and $|y| \leq |\beta|$. □

Proposition 2.6. *Fix* $0 < x \leq \alpha + |\beta|$. *A root of equation* (2.37) *with real part equal to* x *can only exist for*

$$\Delta \leq \frac{1}{x}\log\left(\frac{|\beta|}{x - \alpha}\right)$$

Proof. This follows directly from rearranging the first inequality from (2.39). □

Proposition 2.7. *When a pair of roots of* (2.37) *reach the imaginary axis, they cross transversely from left to right.*

Proof. Let $\Delta_{cr} > 0$ be a delay, for which a pure imaginary root $r = iy_0$ exists. Consider

$$\Delta = \Delta_{cr} + \epsilon, \qquad r = \epsilon x + i(y_0 + \epsilon y). \tag{2.41}$$

Substitute these values into (2.37), separate real and imaginary parts, expand as a power series in ϵ, and use the identities from (2.38) to obtain the equations

$$0 = \Big(x - x\alpha\Delta_{cr} - y_0(y_0 + y\Delta_{cr})\Big)\epsilon + O(\epsilon^2) \tag{2.42}$$

$$0 = \Big(y + xy_0\Delta_{cr} - \alpha(y_0 + y\Delta_{cr})\Big)\epsilon + O(\epsilon^2) \tag{2.43}$$

The $O(\epsilon)$ terms must vanish; solve for x and y to get

$$x = \frac{y_0^2}{(1-\alpha\Delta_{cr})^2 + (y_0\Delta_{cr})^2}, \qquad y = \frac{y_0(\alpha - (y_0^2+\alpha^2)\Delta_{cr})}{(1-\alpha\Delta_{cr})^2 + (y_0\Delta_{cr})^2} \tag{2.44}$$

Clearly $x > 0$, so any root that lies on the imaginary axis at $\Delta = \Delta_{cr}$ crosses into the right half-plane at $\Delta = \Delta_{cr} + \epsilon$. □

Proposition 2.8. *For Equations* (2.2) - (2.3)*, as the delay approaches 0, $\Delta \to 0^+$, there are infinitely many pairs of complex eigenvalues and each pair approaches negative complex infinity.*

Proof. The characteristic equation to the system (2.2) - (2.3) is given by

$$\Phi(\Lambda, \Delta) = \Lambda + \frac{\lambda}{N}\exp(-\Lambda\Delta) + \mu = 0. \tag{2.45}$$

When $\Delta = 0$, there is the only eigenvalue

$$\Lambda = -\frac{\lambda}{N} - \mu. \tag{2.46}$$

When the delay is raised above 0, the characteristic equation becomes transcendental and an infinite sequence of roots is born. Since $\Phi(\Lambda, \Delta)$ is continuous with respect to both Λ and Δ, each eigenvalue Λ must be continuous with respect to Δ. Hence the real part of Λ must go to positive infinity or to negative infinity. However, Proposition (2.5) implies that the eigenvalues cannot come from ∞ on the right side of the complex plane. Therefore all pairs of complex eigenvalues must go to negative complex infinity. □

2.2 Main Steps of Lindstedt's Method

Lindstedt's method was originally formulated for finite-dimensional differential equations, but has been later extended to delay differential equations. Texts such as [35] and [36] apply Lindstedt's method for equations with delays. We synthesize the main steps into four essential parts. These steps provide clarity to the reader who might be unfamiliar with asymptotic techniques and provide a complete methodology for replicating our results for other types of models.

1. We will work with the third order Taylor expansions of the DDEs (2.2) - (2.3), which is given by the Equation (5.173) from Sections 5.1.2 - 5.1.3. We stretch the time and scale our function by $\sqrt{\epsilon}$. This ensures that cubic terms of the function will have one higher order of ϵ than linear terms:

$$\tau = \omega t, \quad \tilde{v}_2(t) = \sqrt{\epsilon}v(t). \tag{2.47}$$

2. We approximate our unknown function $v(t)$, the delay Δ, and the oscillation frequency ω by performing asymptotic expansions in ϵ:

$$v(t) = v_0(t) + \epsilon v_1(t) + ..., \quad \Delta = \Delta_0 + \epsilon\Delta_1 + ..., \quad \omega = \omega_0 + \epsilon\omega_1 + ... \tag{2.48}$$

3. After the expansions given in (2.48) are made, the resulting equation can be separated by the terms with like powers of ϵ (ϵ^0 and ϵ^1). The resulting equations are

$$\mu v_0(\tau) + \tfrac{\lambda}{2} v_0(\tau - \Delta_0\omega_0) + \omega_0 v_0'(\tau) = 0, \tag{2.49}$$

$$\begin{aligned}\mu v_1(\tau) + \tfrac{\lambda}{2} v_1(\tau - \Delta_0\omega_0) + \omega_0 v_1'(\tau) \\ +\omega_1 v_0'(\tau) - \tfrac{1}{24}\lambda v_0^3(\tau - \Delta_0\omega_0) - \tfrac{1}{2}\lambda(\Delta_1\omega_0 + \Delta_0\omega_1) v_0'(\tau - \Delta_0\omega_0) = 0.\end{aligned} \tag{2.50}$$

Equation (2.49) is satisfied by the solution $v_0(\tau) = A_v \sin(\tau)$, which is expected since v_0 describes the queue behavior at the Hopf bifurcation where a limit cycle is born. It can be verified by substitution of $\Delta_0 = \Delta_{cr}$ and $\omega_0 = \omega_{cr}$. Further, the equation for $v_1(\tau)$ has a homogeneous and a non-homogeneous parts to it. The homogeneous part $v_1^H(\tau)$ satisfies an equation which is identical to the Equation (2.49), so any linear combination of $\sin(\tau)$ and $\cos(\tau)$ will satisfy the equation for $v_1^H(\tau)$. To avoid secular terms in the non-homogeneous solution, i.e. terms which grow like τ, the coefficients of $\sin(\tau)$ and $\cos(\tau)$ on the right hand side of Equation (2.50) must vanish.

4. The resulting equations can be solved for A_v and ω_1. Substituting in $\Delta_0 = \Delta_{cr}$ and $\omega_0 = \omega_{cr}$, the results are

$$\omega_1 = -\frac{(\Delta - \Delta_{cr})\lambda^2(\lambda^2 - 4\mu^2)^{3/2}}{4\Big(2\lambda^2\mu - 8\mu^3 + \lambda^2\sqrt{\lambda^2 - 4\mu^2}\arccos(-\frac{2\mu}{\lambda})\Big)}, \tag{2.51}$$

$$A_v(\Delta_1) = \sqrt{\Delta - \Delta_{cr}} \cdot \sqrt{\frac{8(\lambda^2 - 4\mu^2)^2}{2\lambda^2\mu - 8\mu^3 + \lambda^3\sqrt{\lambda^2 - 4\mu^2}\arccos(-\frac{2\mu}{\lambda})}}. \tag{2.52}$$

Amplitude of the Queues

Given the result (2.52), all that is left to do is to trace back through the changes of variables to find the amplitude approximation of queues q_1 and q_2. From Sections 5.1.3 and 5.1.2, we find that as $t \to \infty$, the queues are given up to a phase shift

$$q_1(t) \to \tfrac{\lambda}{2\mu} + w_1(t) \to \frac{\lambda}{2\mu} + \frac{1}{2}A_v \sin(\omega t), \tag{2.53}$$

$$q_2(t) \to \tfrac{\lambda}{2\mu} + w_2(t) \to \frac{\lambda}{2\mu} - \frac{1}{2}A_v \sin(\omega t). \tag{2.54}$$

2.3 Numerical Results of Lindstedt's Method

In this section, we will discuss how well Lindstedt's method fits the behavior of the queueing system. We consider the behavior of the queue lengths throughout time to be determined

with sufficient accuracy by numerical integration of Equations (2.2) - (2.3) using MATLAB's 'dde23' function, so we will test our approximation against the numerical integration results.

We found that Lindstedt's method is highly accurate when the delay is close to the threshold value. In fact, this is evident in every plot of this section. Figures (4) - (5) compare the numerically found amplitude with Lindstedt's amplitude while treating each as a function of delay for parameters $(\lambda, \mu) = (10, 1)$ for the ranges $\Delta \in [\Delta_{cr}, \Delta_{cr} + 0.2]$ and $\Delta \in [\Delta_{cr}, \Delta_{cr} + 1]$, respectively. Lindstedt's amplitude deviates more in the latter plot as there the delay is further from the point of bifurcation, and in both plots the approximation is best when $\tau = \Delta - \Delta_{cr} \to 0$. This is expected because Lindstedt's method perturbs the system about its point of bifurcation, which happens at Δ_{cr}. Hence, as $\Delta \to \Delta_{cr}$, the predicted amplitude must approach the true amplitude. When the gap between delay and critical value increases, however, Lindstedt's method cannot provide theoretical guarantees and in practice the approximation loses accuracy.

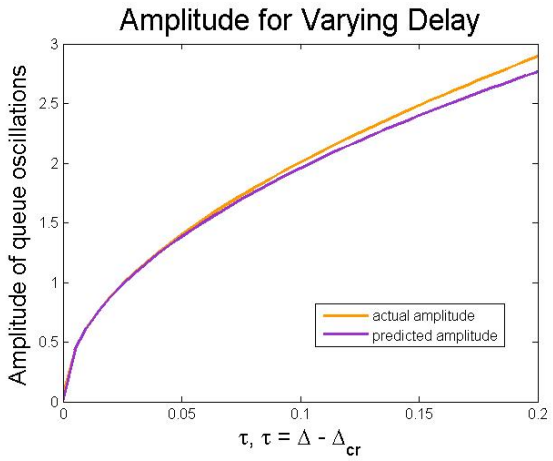

Figure 4: $\lambda = 10$, $\mu = 1$.

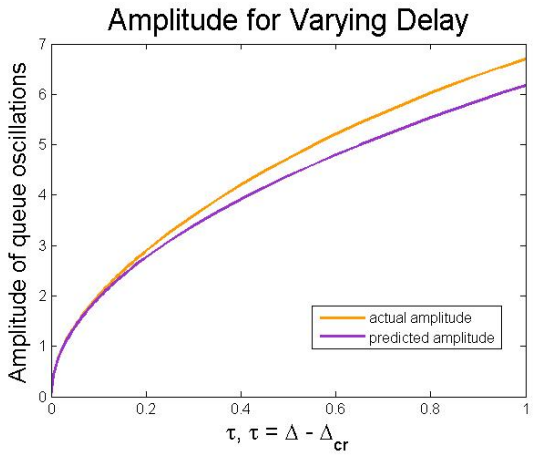

Figure 5: $\lambda = 10$, $\mu = 1$.

An unexpected observation is that the method's performance is affected by the choice of parameters λ and μ. Lindstedt's method works better for smaller λ, which we show in the surface plot in Figure (6) by computing the absolute error of Lindstedt's approximation across a range of λ and Δ. For any delay, Lindstedt's method produces the smallest error when λ is smallest and the error monotonically increases as λ grows. While the absolute error in Figure (6) is constructed for $\mu = 1$, the same holds for other choices of μ. The performance of Lindstedt's method depends on μ in a similar fashion: for each λ and Δ, the method improves in accuracy as μ increases. This trend is exemplified by the surface plot in Figure (7), which shows the absolute error of Lindstedt's method for a fixed λ and varying μ and Δ. For any Δ, the error in approximation monotonically drops as μ increases.

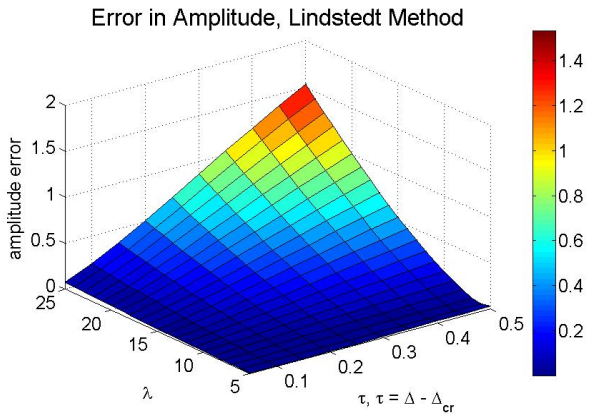

Figure 6: Absolute error, varying λ.

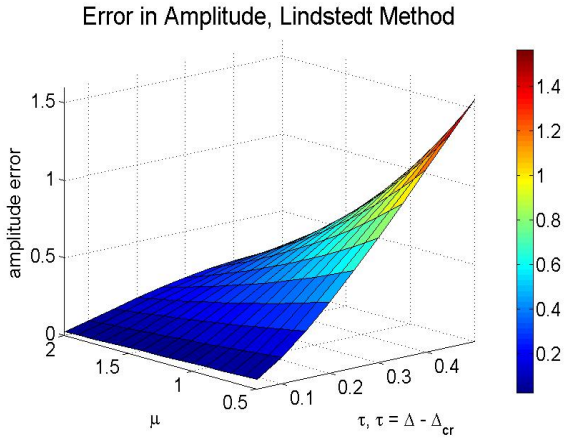

Figure 7: Absolute error, varying μ.

The discovery that Lindstedt's method works differently for different values of λ, μ, and Δ leads to two points. First is that even though the parameters depend on the physical circumstances and can't be easily manipulated, it is beneficial to know when to expect a larger error in approximation even if there are no known analytical error bounds. Second is that seeing the limitations of Lindstedt's method motivated us to try a different approach with the hope of minimizing the error.

2.4 Another Numerical Method (Fitting the Slope Function)

The theory of Hopf bifurcation together with numerical examples highlight that the amplitude is related to the square root of the difference of the actual delay and the critical delay, i.e.

$$\text{Amplitude} \approx C(\lambda, \mu) \cdot \sqrt{\Delta - \Delta_{cr}}, \tag{2.55}$$

where the **slope function** $C(\lambda, \mu)$ depends on the arrival rate λ and the service rate μ. In this section, we propose a statistical way to determine the slope function, which turns out to approximate the amplitude in some cases better than Lindstedt's method.

The Algorithm

For a given pair of parameters λ_1 and μ_1, via numerical integration we find the amplitude $A(\tau)$ for a finite number of points K: $\tau = \Delta - \Delta_{cr} = 0, d, 2d, ..., (K-1)d$ for some $d > 0$. Then $C(\lambda, \mu)$ is such coefficient C that for $A_p = C\sqrt{\tau}$, the error $A_p - A$ is minimized in the least squares sense.

$$C(\lambda, \mu) = \min_{c \in \mathbb{R}} \sum_{j=0}^{K-1} \Big(c\sqrt{jd} - A(jd) \Big)^2 \tag{2.56}$$

When $F(c) = \sum_{j=0}^{K-1} \Big(c\sqrt{jd} - A(jd) \Big)^2$ is minimized at C, $\frac{dF(C)}{dc} = 0$. Hence

$$\frac{dF(C)}{dc} = \sum_{j=0}^{K-1} 2\sqrt{jd} \Big(C\sqrt{jd} - A(jd) \Big) = 0, \tag{2.57}$$

which yields a closed-form solution for C:

$$C = \frac{\sum_{j=0}^{K-1} \sqrt{jd} A(jd)}{\sum_{j=0}^{K-1} jd}. \tag{2.58}$$

This gives us the value of the slope function at (λ_1, μ_1). Figures (8) and (9) show how well the slope function approximates the amplitude compared to Lindstedt's method for $\lambda = 10$ and $\lambda = 20$, respectively.

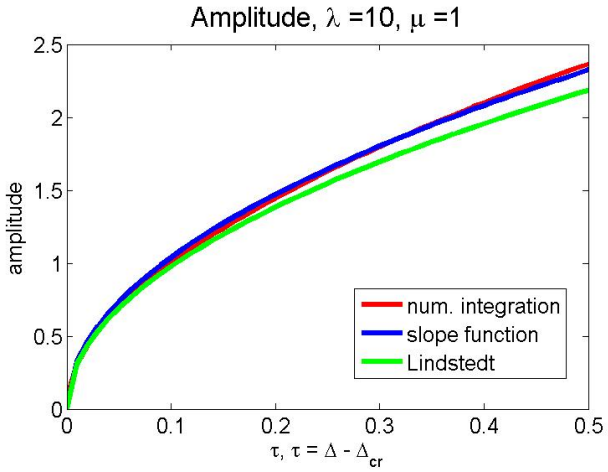

Figure 8: Amplitude predicted by the slope function.

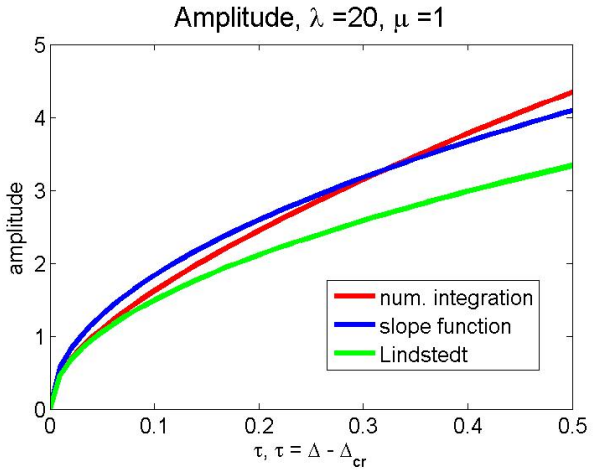

Figure 9: Amplitude predicted by the slope function.

We extrapolate to find the slope function at arbitrary λ and μ based on the function's values computed for a few points. We assume that $C(\lambda, \mu)$ is a separable function,

$$C(\lambda, \mu) = \Lambda(\lambda) M(\mu), \tag{2.59}$$

and then approximate the functions Λ and M by first degree polynomials

$$\Lambda(\lambda) \approx l_0 + l_1 \lambda \tag{2.60}$$
$$M(\mu) \approx m_0 + m_1 \mu. \tag{2.61}$$

We cannot prove that C is a separable function because it depends on the unknown function A that represents the "true" amplitude and it need not be separable. However, the separability assumption is a reasonable approximation because the slope function, as seen from experimental data, indeed is very close to a linear function of λ when μ is kept constant, and it is close to linear as a function of μ while λ is constant. This approximately linear behavior with respect to λ and μ is demonstrated in Figures (10) - (11), respectively, where the blue line in each plot represents the values of $C(\lambda, \mu)$ computed according to Equation (2.58).

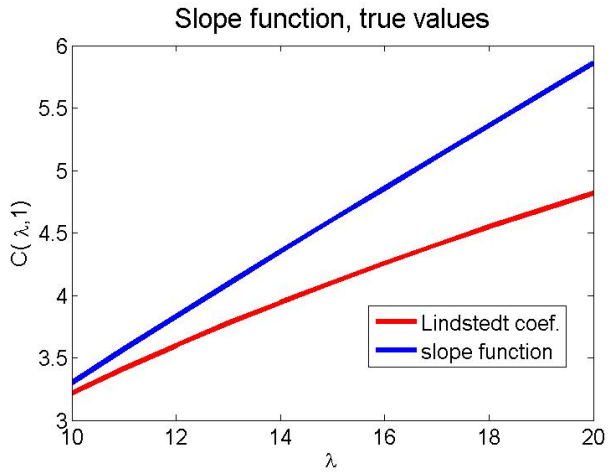

Figure 10: C is approximately linear in λ.

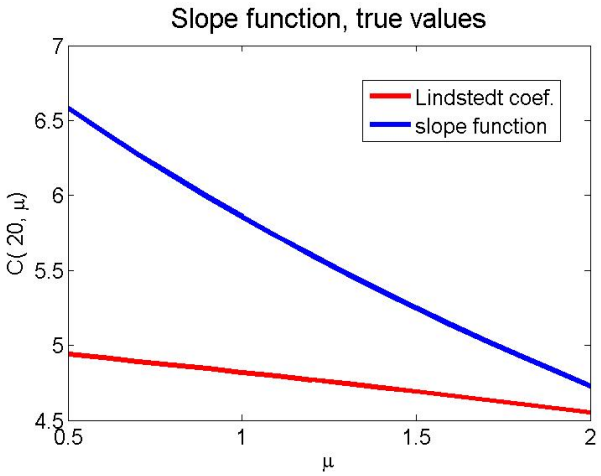

Figure 11: C is approximately linear in μ.

We reduce the number of coefficients from four to three by making the change of variables

$$l_0 = l_{10} l_1, \quad m_0 = m_{10} m_1 \tag{2.62}$$

into Equation (2.59):

$$C(\lambda, \mu) = l_1 m_1 (1_{10} + \lambda)(m_{10} + \mu). \tag{2.63}$$

Here $l_1 m_1$ can be treated as a single coefficient. Determining the three coefficients becomes easy with the function evaluated at three data points: $C(\lambda_1, \mu_1)$, $C(\lambda_2, \mu_1)$, and $C(\lambda_1, \mu_2)$. Equation (2.63) provides equalities that allow us to solve for for the unknown coefficients:

$$\frac{C(\lambda_1, \mu_1)}{C(\lambda_2, \mu_1)} = \frac{l_{10} + \lambda_1}{l_{10} + \lambda_2}, \quad \frac{C(\lambda_1, \mu_1)}{C(\lambda_1, \mu_2)} = \frac{m_{10} + \mu_1}{m_{10} + \mu_2}, \quad l_1 m_1 = \frac{C(\lambda_1, \mu_2)}{(l_{10} + \lambda_1)(m_{10} + \mu_2)} \tag{2.64}$$

In the explicit form, the coefficients of interest are

$$l_{10} = \frac{\lambda_1 - x_1 \lambda_2}{x_1 - 1}, \qquad x_1 = \frac{C(\lambda_1, \mu_1)}{C(\lambda_2, \mu_1)} \tag{2.65}$$

$$m_{10} = \frac{\mu_1 - x_2 \mu_2}{x_2 - 1}, \qquad x_2 = \frac{C(\lambda_1, \mu_1)}{C(\lambda_1, \mu_2)} \tag{2.66}$$

$$l_1 m_1 = \frac{C(\lambda_1, \mu_2)}{(l_{10} + \lambda_1)(m_{10} + \mu_2)}. \tag{2.67}$$

The specific values of coefficients l_{10}, m_{10}, and $l_1 m_1$ will slightly vary depending on which parameters λ_1, λ_2, μ_1, and μ_2 are chosen because the linearity assumption of Equations (2.60) - (2.61) is only an approximation of the true behavior as shown in Figures (10) - (11). Hence, for optimal results one should choose the data points $C(\lambda_1, \mu_1)$, $C(\lambda_2, \mu_1)$, and $C(\lambda_1, \mu_2)$ around the range of λ and μ that one is interested in.

2.5 Numerical Results for Fitting the Slope Function

Figures (12) and (13) show the absolute error of the amplitude resulting from the slope function (plot on the left) and Lindstedt's method (plot on the right) for varying λ and Δ. Note

that overall the slope function results in a smaller error for a wide range of λ and Δ, with a maximum error of 0.4 compared with 1.5 maximum error in Lindstedt's approximation. However, unlike Lindstedt's technique the slope function no longer guarantees to be accurate when Δ approaches Δ_{cr}. Thus, it is advantageous to use the slope function for predicting the amplitude when the delay is sufficiently greater than the critical value, while Lindstedt's method is preferable when the delay is close to the threshold. A similar observation holds in the case when λ is constant and μ varies. Surface plots (14) and (15) show that the slope function has a maximum error of less than a third of the error seen in Lindstedt's method, being outperformed only when the delay approaches the critical value.

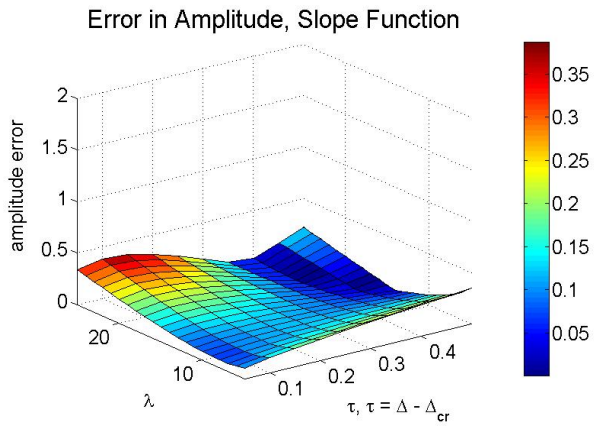

Figure 12: Absolute error from the slope function, with $\mu = 1$.

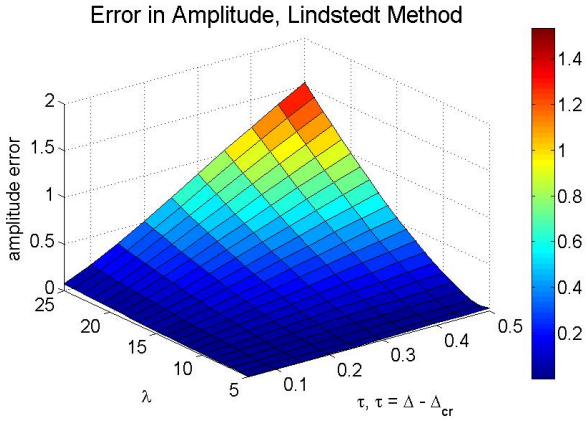

Figure 13: Absolute error from Lindtsedt's method, with $\mu = 1$.

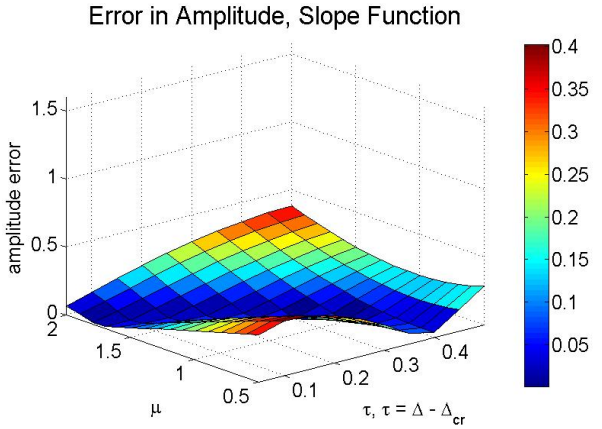

Figure 14: Absolute error from the slope function, with $\lambda = 20$.

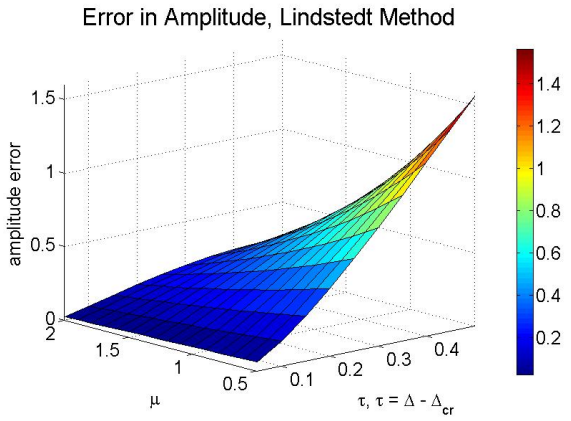

Figure 15: Absolute error from Lindtsedt's method, with $\lambda = 20$.

3 Moving Average Fluid Model

In this section, we present a model similar to the constant delay model from Section 2, except here, the information given to the customer is the moving average of the queue lengths. Figure (1) still accurately represents the overall system: the customers appear at a rate λ, join one of the two queues with probabilities p_1 and p_2, and get service at a rate μ with an infinite number of servers. However, the customers are informed about the *average* queue length found between the current time and Δ time units in the past. Customers join the queues according to the Multinomial Logit Model,

$$p_1 = \frac{\exp\Big(-\frac{1}{\Delta}\int_{t-\Delta}^{t} q_1(s)ds\Big)}{\exp\Big(-\frac{1}{\Delta}\int_{t-\Delta}^{t} q_1(s)ds\Big) + \exp\Big(-\frac{1}{\Delta}\int_{t-\Delta}^{t} q_2(s)ds\Big)} \tag{3.68}$$

$$p_2 = \frac{\exp\Big(-\frac{1}{\Delta}\int_{t-\Delta}^{t} q_2(s)ds\Big)}{\exp\Big(-\frac{1}{\Delta}\int_{t-\Delta}^{t} q_1(s)ds\Big) + \exp\Big(-\frac{1}{\Delta}\int_{t-\Delta}^{t} q_2(s)ds\Big)}, \tag{3.69}$$

where p_i is the probability of i^{th} queue being joined, $q_i(t)$ is the i^{th} queue length, and the integral expressions in the exponents are the moving averages of the queues.

Given these probabilities we can describe the queue lengths as

$$\dot{q}_1 = \lambda \cdot \frac{\exp\Big(-\frac{1}{\Delta}\int_{t-\Delta}^{t} q_1(s)ds\Big)}{\exp\Big(-\frac{1}{\Delta}\int_{t-\Delta}^{t} q_1(s)ds\Big) + \exp\Big(-\frac{1}{\Delta}\int_{t-\Delta}^{t} q_2(s)ds\Big)} - \mu q_1(t) \tag{3.70}$$

$$\dot{q}_2 = \lambda \cdot \frac{\exp\Big(-\frac{1}{\Delta}\int_{t-\Delta}^{t} q_2(s)ds\Big)}{\exp\Big(-\frac{1}{\Delta}\int_{t-\Delta}^{t} q_1(s)ds\Big) + \exp\Big(-\frac{1}{\Delta}\int_{t-\Delta}^{t} q_2(s)ds\Big)} - \mu q_2(t), \tag{3.71}$$

where $\Delta, \lambda, \mu > 0$. The equations are simplified by notation for the moving average m_i, which itself satisfies a delay differential equation:

$$m_i(t,\Delta) = \frac{1}{\Delta}\int_{t-\Delta}^{t} q_i(s)ds, \tag{3.72}$$

$$\dot{m}_i(t,\Delta) = \frac{1}{\Delta}\cdot\big(q_i(t) - q_i(t-\Delta)\big), \quad i \in \{1,2\}. \tag{3.73}$$

The Moving Average model can now be described by the equations

$$\dot{q}_1 = \lambda \cdot \frac{\exp(-m_1(t))}{\exp(-m_1(t)) + \exp(-m_2(t))} - \mu q_1(t) \tag{3.74}$$

$$\dot{q}_2 = \lambda \cdot \frac{\exp(-m_2(t))}{\exp(-m_1(t)) + \exp(-m_2(t))} - \mu q_2(t) \tag{3.75}$$

$$\dot{m}_1 = \frac{1}{\Delta}\cdot(q_1(t) - q_1(t-\Delta)) \tag{3.76}$$

$$\dot{m}_2 = \frac{1}{\Delta}\cdot(q_2(t) - q_2(t-\Delta)). \tag{3.77}$$

Since the functions m_i represent the averages of q_i, the initial conditions of m_i must reflect this. With $f_1(t)$ and $f_2(t)$ being continuous and nonnegative functions on $t \in [-\Delta, 0]$, the initial conditions are

$$q_1(t) = f_1(t), \quad q_2(t) = f_2(t), \quad t \in [-\Delta, 0]; \tag{3.78}$$

$$m_1(0) = \frac{1}{\Delta}\int_{t-\Delta}^{t} f_1(s)ds, \quad m_2(0) = \frac{1}{\Delta}\int_{t-\Delta}^{t} f_2(s)ds. \tag{3.79}$$

3.1 Hopf Bifurcation in the Moving Average Model

The behavior of the queues (3.74) - (3.77) depends on the delay parameter Δ, but the dependence itself is more nuanced than in the Constant Delay model. When the delay is sufficiently small **or sufficiently large**, all eigenvalues have negative real parts, so the queue lengths converge to a unique and stable equilibrium:

$$q_i(t) \;\; \rightarrow \;\; \frac{\lambda}{2\mu}. \tag{3.80}$$

Theorem (3.1) proves the existence and uniqueness of equilibrium $\frac{\lambda}{2\mu}$, and states the conditions for which the equilibrium is stable.

As the delay increases, the complex pairs of eigenvalues move from negative complex infinity towards the imaginary axis. For given parameters λ and μ, finitely many pairs of complex eigenvalue may cross (one by one) to the positive side of the imaginary axis. At each critical delay Δ_{cr} where a pair of eigenvalues crosses the imaginary axis, a supercritical Hopf bifurcation occurs. Theorems (3.2) and (3.3) prove these results. Unlike in the Constant Delay model, however, as the delay continues to increase each pair of the complex eigenvalues will cross back to the negative side of imaginary axis, crossing in the "last in first out" order (the first pair of eigenvalues to cross the imaginary axis in the positive direction is the last to cross in the negative direction). Figure (16) illustrates the behavior. The curves Hopf 1 and Hopf 2 indicate where the Hopf bifurcations occur due to the first and second pairs of eigenvalues, respectively. For a fixed λ, as Δ increases, the first time a Hopf curve crosses λ is when a limit cycle is born, and the second time the same Hopf curve crosses λ is where that limit cycle disappears. The non-Hopf curve given by $\frac{\lambda}{\Delta} - \mu^2 = 0$ is the boundary past which the Hopf curves cannot cross (and thus a Hopf bifurcation cannot occur). This is shown in Proposition (3.4). The orange line given by $\lambda = 2\mu^2\Delta + 2\mu$ indicates the direction in which the eigenpairs move relative to Δ. For fixed values of λ and μ, every complex eigenpair moves in the real $+\infty$ direction as delay increases up to the orange line, and afterwards all eigenpairs move in the reverse direction as delay increases further. The orange line also passes through the minimum of each Hopf curve, since the minima represent an eigenpair that reaches the imaginary axis at $\Delta = \frac{\lambda - 2\mu}{2\mu^2}$, and then reverts the direction back to $-\infty$ without crossing the imaginary axis. As shown in Theorem (3.2), a bifurcation does not occur at the minima of the Hopf curves.

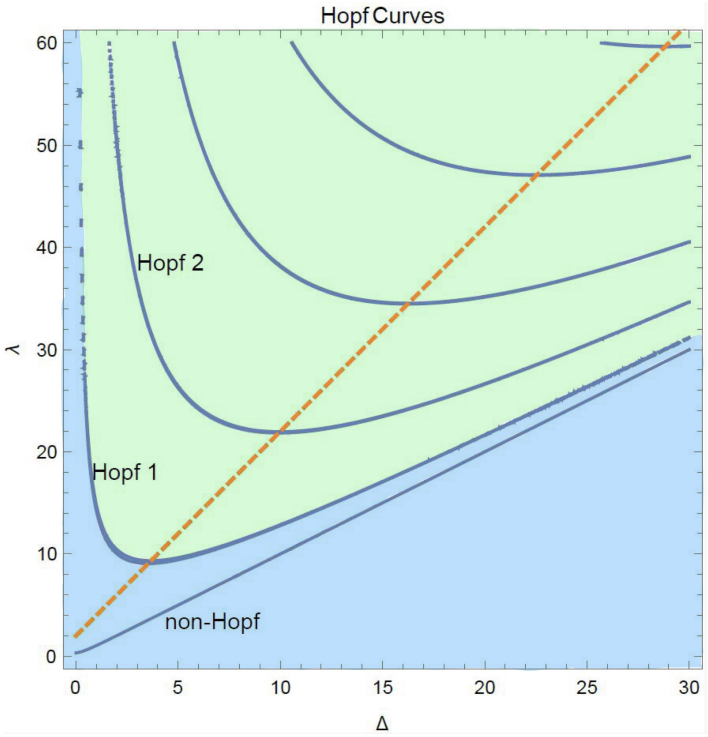

Figure 16: The Hopf curves for $\mu = 1$; green area - limit cycles; blue area - stable equilibrium.

To determine Δ_{cr} where the Hopf bifurcations occur, we linearize the system of Equations (3.74) - (3.77) and separate the variables. Sections 5.3 and 5.4 show this in detail, and the resulting system of equations is

$$\dot{\tilde{v}}_2 = -\frac{\lambda}{2}\tilde{v}_4(t) - \mu\tilde{v}_2(t) \tag{3.81}$$

$$\dot{\tilde{v}}_4 = \frac{1}{\Delta}\Big(\tilde{v}_2(t) - \tilde{v}_2(t-\Delta)\Big). \tag{3.82}$$

Under the assumption that $\tilde{v}_2 = e^{\Lambda t}$, $\Lambda \neq 0$, the characteristic equation is

$$\Phi(\Lambda) = \Lambda + \mu + \frac{\lambda}{2\Delta\Lambda} - \frac{\lambda}{2\Delta\Lambda}\cdot e^{-\Lambda\Delta} = 0. \tag{3.83}$$

If $\Lambda = i\omega_{cr}$, $\omega_{cr} > 0$, then the characteristic equation gives the equalities

$$\sin(\omega_{cr}\Delta_{cr}) = -\frac{2\Delta_{cr}\mu\omega_{cr}}{\lambda}, \quad \cos(\omega_{cr}\Delta_{cr}) = 1 - \frac{2\Delta_{cr}\omega_{cr}^2}{\lambda}. \tag{3.84}$$

From the trigonometric identity $\sin^2(\omega_{cr}\Delta_{cr}) + \cos^2(\omega_{cr}\Delta_{cr}) = 1$, ω_{cr} can be found

$$\omega_{cr} = \sqrt{\frac{\lambda}{\Delta_{cr}} - \mu^2}. \tag{3.85}$$

Since we assumed ω_{cr} to be real and positive, the condition $\frac{\lambda}{\Delta_{cr}} - \mu^2 > 0$ must hold. When ω_{cr} is substituted into Equation (3.84), the transcendental equation for Δ_{cr} is attained

$$\sin\left(\Delta_{cr}\cdot\sqrt{\frac{\lambda}{\Delta_{cr}} - \mu^2}\right) + \frac{2\mu\Delta_{cr}}{\lambda}\cdot\sqrt{\frac{\lambda}{\Delta_{cr}} - \mu^2} = 0. \tag{3.86}$$

When Δ exceeds the **smallest nonnegative root** of Equation (3.86), the stability of equilibrium is lost and a stable limit cycle emerges. Figures (17) and (18) show the transition. Theorem (3.2) shows that a Hopf bifurcation occurs at every root Δ_{cr}, such that $\Delta_{cr} \neq \frac{\lambda-2\mu}{2\mu^2}$. Theorem (3.3) proves the stability of the emergent limit cycles.

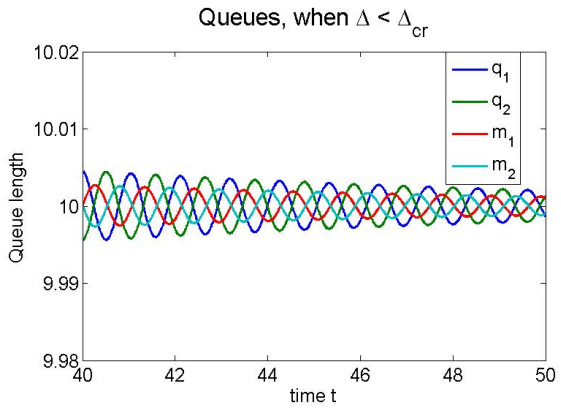

Figure 17: Before bifurcation.

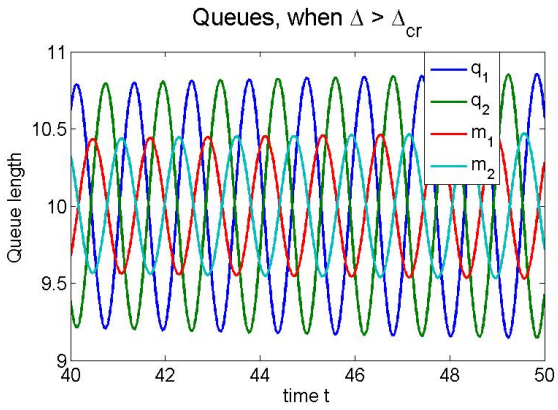

Figure 18: After bifurcation.

Theorem 3.1. *Suppose Equation* (3.86) *has no roots* $\Delta_{cr} > 0$. *Then Equations* (3.74) - (3.77) *have a unique and stable equilibrium for all* $\Delta > 0$.

Suppose there exists $\Delta_{cr} > 0$ *satisfying Equation* (3.86). *Then Equations* (3.74) - (3.77) *have a unique stable equilibrium when* Δ *is less than the smallest positive root or greater than the largest root of Equation* (3.86). *Further, the largest root is less than* $\frac{\lambda}{\mu^2}$.

The unique steady state solution to Equations (3.74) - (3.77) *is given by*

$$q_1^*(t) = q_2^*(t) = m_1^*(t) = m_2^*(t) = \frac{\lambda}{2\mu}. \tag{3.87}$$

Proof. See the proof in Appendix. □

Theorem 3.2. *If* Δ_{cr} *satisfies Equation* (3.86) *and* $\Delta_{cr} \neq \frac{\lambda-2\mu}{2\mu^2}$, *then the queues from Equations* (3.74) - (3.77) *undergo a Hopf bifurcation at* Δ_{cr}.

Proof. For each Δ_{cr} satisfying Equation (3.86), the characteristic equation (3.83) has two simple roots $\Lambda = \pm i\omega_{cr}$. Further, through implicit differentiation of Equation (3.83), it can be shown that $\mathrm{Re}[\Lambda'(\Delta_{cr})] \neq 0$:

$$\mathrm{Re}\ \Lambda'(\Delta_{cr}) = \frac{2\omega_{cr}^2(\lambda - 2\mu - 2\mu^2\Delta_{cr})}{4\omega_{cr}^2\Delta_{cr}(3 + 2\Delta_{cr}\mu) + \lambda(4 + \Delta_{cr}\lambda + 4\Delta_{cr}\mu)}, \tag{3.88}$$

which is nonzero because the denominator is positive, and the assumption $\Delta_{cr} \neq \frac{\lambda-2\mu}{2\mu^2}$ guarantees the numerator to be nonzero. Further, all other eigenvalues Λ^* are complex with a nonzero real part, so $\Lambda^* \neq m\Lambda$. Therefore, a Hopf bifurcation occurs at Δ_{cr}. This Theorem suggests that there may be multiple Hopf bifurcations for parameters λ and μ. □

Theorem 3.3. *A Hopf bifurcation given by Theorem* (3.2) *is supercritical.*

Proof. We will use the method of slow flow to determine whether the limit cycle is stable. The third order expansion of Equations (3.74) - (3.75) can be uncoupled, and the resulting equations of interest are given by Sections 5.3 and 5.4:

$$\dot{\tilde{v}}_2 = \lambda\Big(- \frac{\tilde{v}_4(t)}{2} + \frac{\tilde{v}_4(t)^3}{24}\Big) - \mu\tilde{v}_2(t) \tag{3.89}$$

$$\dot{\tilde{v}}_4 = \frac{1}{\Delta}\Big(\tilde{v}_2(t) - \tilde{v}_2(t-\Delta)\Big). \tag{3.90}$$

The two variables are scaled by $\sqrt{\epsilon}$

$$\tilde{v}_2(t) = \sqrt{\epsilon}v(t), \qquad \tilde{v}_4(t) = \sqrt{\epsilon}u(t), \tag{3.91}$$

the delay and the frequency are expanded close to their critical values, and two time scales are introduced:

$$\Delta = \Delta_{cr} + \epsilon\alpha, \quad \omega = \omega_{cr} + \epsilon\beta, \quad \xi = \omega t, \quad \eta = \epsilon t. \tag{3.92}$$

The functions $v(t)$ and $u(t)$ are also expanded

$$v(\xi,\eta) = v_0(\xi,\eta) + \epsilon v_1(\xi,\eta) \tag{3.93}$$

$$u(\xi,\eta) = u_0(\xi,\eta) + \epsilon u_1(\xi,\eta). \tag{3.94}$$

We introduce the form for $v_0(\xi,\eta)$

$$v_0(\xi,\eta) = A(\eta)\cos(\xi) + B(\eta)\sin(\xi), \tag{3.95}$$

which allows us to find the form of $u_0(\xi,\eta)$:

$$u_0(\xi,\eta) = -\frac{2(A(\eta) + B(\eta)\omega_{cr})}{\lambda}\cos(\xi) - \frac{2(B(\eta) - A(\eta)\omega_{cr})}{\lambda}\sin(\xi). \tag{3.96}$$

The variables v_0 and u_0 can now be substituted in their explicit form into the equations for $\dot{v}(t)$ and $\dot{u}(t)$. When the like orders of ϵ are collected, the zeroth order terms vanish, as expected. The terms involving the first order of ϵ comprise of (i) the differential operator acting on x_1, (ii) the non-resonant terms $\cos(3\xi)$ and $\sin(3\xi)$, and (iii) the resonant terms involving $\cos(\xi)$ and $\sin(\xi)$. For no secular terms, the coefficients of $\cos(\xi)$ and $\sin(\xi)$ must vanish, giving a slow flow on $A(\eta)$ and $B(\eta)$. By introducing the polar coordinates

$$A = R\cos(\Theta), \qquad B = R\sin(\Theta) \tag{3.97}$$

we find equation for the radial component $\frac{d}{d\eta}R(\eta)$

$$\frac{dR}{d\eta} = \frac{R(\lambda - \Delta_{cr}\mu^2)(R^2(\lambda+2\mu) - 4\alpha\lambda(\lambda - 2\mu - 2\Delta_{cr}\mu^2))}{2\Delta_{cr}\lambda(-\Delta_{cr}\lambda^2 + 4\Delta_{cr}\mu^2(3 + 2\Delta_{cr}\mu) - 4\lambda(4 + 3\Delta_{cr}\mu))} \tag{3.98}$$

Assuming $R \geq 0$, the equilibrium points are

$$R_0 = 0, \quad R_1 = \sqrt{\frac{4\alpha\lambda(\lambda - 2\mu - 2\Delta_{cr}\mu^2)}{\lambda + 2\mu}}. \tag{3.99}$$

From Theorem (3.2), $\Delta_{cr} \neq \frac{\lambda-2\mu}{2\mu^2}$. The condition $\Delta_{cr} < \frac{\lambda-2\mu}{2\mu^2}$ is equivalent to Δ_{cr} being the lower critical value for a fixed λ, i.e. being on the left branch of the Hopf curve (see Figure (16)). When on the left side of the Hopf, α must be positive for R_1 to be real. In other words, the limit cycle is born as Δ increases. On the other hand, if $\Delta_{cr} > \frac{\lambda-2\mu}{2\mu^2}$ then we are on the right side of the Hopf curve, and α must be negative for R_1 to be real. Hence the limit cycle appears as Δ decreases. In both cases, the assumption $\frac{\lambda}{\Delta_{cr}} - \mu^2 > 0$ that arose from the frequency ω_{cr} being positive, guarantees that $\frac{dR}{d\eta}$ is positive on the interval $R \in (0, R_1)$ and negative when $R > R_1$. Therefore the Hopf bifurcation is supercritical.

□

Proposition 3.4. *The characteristic equation* (3.83) *cannot have a purely imaginary eigenvalue when* $\lambda \leq \mu^2\Delta$.

Proof. Equation (3.85) shows that when an eigenvalue $\Lambda = a+ib$ reaches the imaginary axis, i.e. $a = 0$, the imaginary part is given by $b = \pm\omega_{cr} = \pm\sqrt{\frac{\lambda}{\Delta} - \mu^2} \in \mathbb{R}$. Hence the condition $\frac{\lambda}{\Delta} - \mu^2 > 0$ must hold.

Any point on a Hopf curve from Figure (16) indicates an existence of a purely imaginary solution to the characteristic equation. This implies that the Hopf curves must stay to the left of the non-Hopf curve, which is given by $\lambda = \mu^2\Delta$. □

Proposition 3.5. *Any real nontrivial eigenvalue of the Equation* (3.83) *is negative.*

Proof. Under the assumption $\Lambda \neq 0$ and $\Lambda \in \mathbb{R}$, the characteristic equation can be rewritten as

$$1 + \frac{2\Delta}{\lambda} \cdot \Lambda(\Lambda + \mu) = e^{-\Lambda\Delta}. \tag{3.100}$$

The left hand side (LHS) and the right hand side (RHS) intersect at $\Lambda = 0$, and for $\Lambda > 0$ the LHS is monotonically increasing while the RHS is monotonically decreasing. Hence when $\Lambda \in \mathbb{R}$, this equality can only hold for $\Lambda < 0$. □

Proposition 3.6. *If* $\Delta > \frac{\lambda}{\mu^2}$, *then any complex eigenvalue of the Equation* (3.83) *has a negative real part.*

Proof. We will argue by contradiction. Assume that $\Delta > \frac{\lambda}{\mu^2}$ and $a \geq 0$ for some $\Lambda = a + ib$ where $a, b \in \mathbb{R}$. We substitute Λ into Equation (3.83) and separate the real and imaginary parts:

$$\cos(b\Delta)e^{-a\Delta}\lambda = 2a^2\Delta - 2b^2\Delta + \lambda + 2a\mu\Delta \tag{3.101}$$

$$\sin(b\Delta)e^{-a\Delta}\lambda = -2b\Delta(2a + \mu). \tag{3.102}$$

Summing the squares of the two equations, we get

$$e^{-2a\Delta}\lambda^2 = \big(2a^2\Delta - 2b^2\Delta + \lambda + 2a\mu\Delta\big)^2 + \big(2b\Delta(2a + \mu)\big)^2, \tag{3.103}$$

and after some algebra we find

$$b^2 \leq \frac{1}{\Delta}(\lambda + 2a\mu\Delta + 2a^2\Delta) - (2a+\mu)^2 \tag{3.104}$$

$$= \frac{\lambda}{\Delta} - \mu^2 - 2a(a+\mu) < -2a(a+\mu) \leq 0, \tag{3.105}$$

so $b \notin \mathbb{R}$, and we get a contradiction. Therefore $\mathrm{Re}[\Lambda] = a < 0$ when $\Delta > \frac{\lambda}{\mu^2}$. □

Proposition 3.7. *Let $\lambda, \mu, \Delta > 0$. There exists $\Delta^* > 0$ such that for any $\Delta < \Delta^*$, all complex eigenvalues of the characteristic equation* (3.83) *have negative real parts.*

Proof. Let $\Lambda = a + ib$ be a solution of Equation (3.83). Then a and b must satisfy

$$\cos(b\Delta) = \frac{e^{a\Delta}}{\lambda}(2a^2\Delta - 2b^2\Delta + \lambda + 2a\mu\Delta) \tag{3.106}$$

$$\sin(b\Delta) = -\frac{e^{a\Delta}}{\lambda} \cdot 2b\Delta(2a+\mu). \tag{3.107}$$

If b satisfies these equations, then $-b$ is a solution too. Hence WLOG we will assume that $b > 0$. Summing the squares of the two equations, we get

$$e^{-2a\Delta}\lambda^2 = \big(2a^2\Delta - 2b^2\Delta + \lambda + 2a\mu\Delta\big)^2 + \big(2b\Delta(2a+\mu)\big)^2, \tag{3.108}$$

from which b can be expressed as a *continuous* function of a and Δ, namely $b(a, \Delta)$. If $a = 0$ then $b(0, \Delta) = \sqrt{\frac{\lambda}{\Delta} - \mu^2}$, and when plugged into Equation (3.107) we get

$$\sin(b(0,\Delta)\Delta) = -\frac{2\mu}{\lambda} \cdot b(0,\Delta)\Delta \tag{3.109}$$

$$\sin(x(0,\Delta)) = -\frac{2\mu}{\lambda} \cdot x(0,\Delta) \tag{3.110}$$

$$x(a,\Delta) = b(a,\Delta)\Delta, \quad x(0,\Delta) = \Delta\sqrt{\frac{\lambda}{\Delta} - \mu^2}. \tag{3.111}$$

The function x will be helpful in the proof. Note that since x is a continuous function of b and therefore of a. Let us define $\Delta^* > 0$ as

$$\Delta^* = \begin{cases} \frac{\lambda}{2\mu^2}, & \frac{\lambda}{2\mu} \leq \pi \\ \frac{\lambda - \sqrt{\lambda^2 - 4\mu^2\pi^2}}{2\mu^2}, & \text{otherwise.} \end{cases} \tag{3.112}$$

This choice of Δ^* guarantees that for all $\Delta < \Delta^*$, the functions $b(0, \Delta)$ and $x(0, \Delta)$ are real. Further, Δ^* ensures that $0 < x(0, \Delta) < \min(\pi, \frac{\lambda}{2\mu})$ for all $\Delta < \Delta^*$, which can be checked from Equation (3.111). The condition $0 < x(0, \Delta) < \pi$ implies that

$$\sin(x(0,\Delta)) > 0 > -\frac{2\mu}{\lambda} \cdot x(0,\Delta). \tag{3.113}$$

However, for any $a \geq 0$, Equation (3.107) gives the inequality

$$\sin(x(a,\Delta)) = -\frac{e^{a\Delta}}{\lambda} \cdot 2x(a,\Delta)(2a+\mu) \leq -\frac{2\mu}{\lambda} \cdot x(a,\Delta), \tag{3.114}$$

By the continuity of $x(a, \Delta)$ with respect to a then

$$\sin(x(0, \Delta)) \leq -\frac{2\mu}{\lambda} \cdot x(0, \Delta), \tag{3.115}$$

which is in contradiction with Equation (3.113). Hence a must be negative to satisfy the characteristic equation for $\Delta < \Delta^*$.

□

To quantitatively describe the queue behavior after the bifurcation, we will determine an approximation to the amplitude A of the queues via Lindstedt's method. From the trigonometric identity

3.2 Lindstedt's Method

To find the amplitude of oscillations, we apply Lindstedt's method according to the steps shown in Subsection 2.2. However, instead of working with one unknown function we are now working with two.

1. We stretch the time and scale both functions by $\sqrt{\epsilon}$:

$$\tau = \omega t, \quad \tilde{v}_2 = \sqrt{\epsilon} v(t), \quad \tilde{v}_4 = \sqrt{\epsilon} u(t). \tag{3.116}$$

   This ensures that the cubic terms will have one higher order of ϵ than linear terms. The new equations are of the form

$$\begin{aligned} \omega v'(\tau) &= \lambda\Big(-\frac{u(\tau)}{2} + \frac{\epsilon u(\tau)^3}{24} \Big) - \mu v(\tau) && (3.117) \\ \omega u'(\tau) &= \frac{1}{\Delta}\Big(v(\tau) - v(\tau - \omega\Delta) \Big). && (3.118) \end{aligned}$$

2. We approximate the variables by performing asymptotic expansions in ϵ:

$$\begin{aligned} v(t) &= v_0(t) + \epsilon v_1(t) + ... && (3.119) \\ u(t) &= u_0(t) + \epsilon u_1(t) + ... && (3.120) \\ \Delta &= \Delta_0 + \epsilon \Delta_1 + ... && (3.121) \\ \omega &= \omega_0 + \epsilon \omega_1 + ... && (3.122) \end{aligned}$$

3. We substitute Equations (3.119) - (3.122) into Equations (3.117) - (3.118) and separate each of the resulting equations into two equations by collecting all the terms of the like powers of ϵ. The terms of order ϵ^0 yield

$$\begin{aligned} 0 &= \frac{1}{2}\lambda m_0(\tau) + \mu v_0(\tau) + \omega_0 v_0'(\tau) && (3.123) \\ 0 &= -v_0(\tau) + v_0(\tau - \Delta_0\omega_0) + \Delta_0\omega_0 m_0'(\tau), && (3.124) \end{aligned}$$

and the terms of order ϵ^1 yield

$$\begin{aligned} 0 &= -\frac{1}{24}\lambda m_0(\tau)^3 + \frac{1}{2}\lambda m_1(\tau) + \mu v_1(\tau) + \omega_1 v_0'(\tau) + \omega_0 v_1'(\tau) \qquad (3.125) \\ 0 &= \Delta_1\Big(v_0(\tau) - v_0(\tau - \Delta_0\omega_0)\Big) + \Delta_0^2\omega_1 m_0'(\tau) + \Delta_0^2\omega_0 m_1'(\tau) \\ &- \Delta_0\Big(v_1(\tau) - v_1(\tau - \Delta_0\omega_0) + (\Delta_1\omega_0 + \Delta_0\omega_1)v_0'(\tau - \Delta_0\omega_0)\Big). \qquad (3.126) \end{aligned}$$

Equations (3.123) - (3.125) give expressions for the following functions:

$$m_0(\tau) = -\frac{2}{\lambda}\Big(\mu v_0(\tau) + \omega_0 v_0'(\tau)\Big) \qquad (3.127)$$

$$m_1(\tau) = -\frac{2}{\lambda}\left(\frac{\big(\mu v_0(\tau) + \omega_0 v_0'(\tau)\big)^3}{3\lambda^2} + \mu v_1(\tau) + \omega_1 v_0'(\tau) + \omega_0 v_1'(\tau)\right) \qquad (3.128)$$

$$v_0(\tau - \Delta_0\omega_0) = v_0(\tau) + \frac{2\Delta_0\omega_0}{\lambda}\Big(\mu v_0'(\tau) + \omega_0 v_0''(\tau)\Big) \qquad (3.129)$$

4. To solve for v_0 we substitute Equation (3.127) into Equation (3.124)

$$0 = -v_0(\tau) + v_0(\tau - \Delta_0\omega_0) - \frac{2\Delta_0\omega_0}{\lambda}\Big(\mu v_0'(\tau) + \omega_0 v_0''(\tau)\Big) \qquad (3.130)$$

and it can be verified that the the solution $v_0(\tau)$ takes the periodic form

$$v_0(\tau) = A_v \sin\tau. \qquad (3.131)$$

This is expected since v_0 describes the behavior at the Hopf bifurcation.

5. The remaining unknown function is v_1. Its delay-differential equation has a homogeneous and a non-homogeneous part to it, namely $v_1(\tau) = v_1^H(\tau) + v_1^N(\tau)$. We find the equation for v_1^H by setting all other functions to zero

$$0 = -v_1(\tau) + v_1(\tau - \Delta_0\omega_0) - \frac{2\Delta_0\omega_0}{\lambda}\Big(\mu v_1'(\tau) + \omega_0 v_1''(\tau)\Big), \qquad (3.132)$$

which is identical to the differential equation (3.130) that describes v_0. Hence the solution for $v_1^H(\tau)$ is of the form

$$v_1^H(\tau) = a_1\sin(\tau) + b_1\cos(\tau), \qquad (3.133)$$

and any terms with $\sin(\tau)$ and $\cos(\tau)$ will produce secular terms in the nonhomogeneous solution to v_1. Equations (3.134) and (3.135) eliminate the coefficients of the sine and cosine terms, respectively:

$$\begin{aligned} &4A_v\Delta_1\lambda^2\omega_0^2 + A_v^3\Delta_0\mu^2\omega_0^2 + A_v^3\Delta_0\omega_0^4 + 8A_v\Delta_0\lambda^2\omega_0\omega_1 \\ &-2A_v\Delta_1\lambda^3\omega_0\sin(\Delta_0\omega_0) - 2A_v\Delta_0\lambda^3\omega_1\sin(\Delta_0\omega_0) = 0 \qquad (3.134) \\ &4A_v\Delta_1\lambda^2\mu\omega_0 + A_v^3\Delta_0\mu^3\omega_0 + A_v^3\Delta_0\mu\omega_0^3 + 4A_v\Delta_0\lambda^2\mu\omega_1 \\ &+2A_v\Delta_1\lambda^3\omega_0\cos(\Delta_0\omega_0) + 2A_v\Delta_0\lambda^3\omega_1\cos(\Delta_0\omega_0) = 0 \qquad (3.135) \end{aligned}$$

6. Δ_0, ω_0, and $\Delta_1 = \Delta - \Delta_{cr}$ are known, so we find

$$\omega_1 = -\frac{4\Delta_1\lambda^2\mu\omega_0 + A_v^2\Delta_0\mu^3\omega_0 + A_v^2\Delta_0\mu\omega_0^3 + 2\Delta_1\lambda^3\omega_0\cos(\Delta_0\omega_0)}{2\Delta_0\lambda^2\Big(2\mu + \lambda\cos(\Delta_0\omega_0)\Big)} \tag{3.136}$$

$$A_v(\Delta_1) = 2\sqrt{\Delta_1}\cdot\sqrt{-2\lambda^2\mu\omega_{cr} - \lambda_3\omega_{cr}\cos(\Delta_{cr}\omega_{cr})}\cdot\Big(\Delta_{cr}(\mu^2+\omega_0^2)\Big)^{-\frac{1}{2}}$$
$$\cdot\Big(2\mu\omega_0 - \lambda\omega_0\cos(\Delta_{cr}\omega_{cr}) - \lambda\mu\sin(\Delta_{cr}\omega_{cr})\Big)^{-\frac{1}{2}}. \tag{3.137}$$

Amplitude of the Queues

The function A_v approximates the amplitude of oscillations for the function $v(t)$. When translated into the original variables, the amplitude of queues as $t \to \infty$ is

$$q_1(t) \to \ \tfrac{\lambda}{2\mu} + w_1(t) \to \ \frac{\lambda}{2\mu} + \frac{1}{2}A_v\sin(\omega t) \tag{3.138}$$

$$q_2(t) \to \ \tfrac{\lambda}{2\mu} + w_2(t) \to \ \frac{\lambda}{2\mu} - \frac{1}{2}A_v\sin(\omega t). \tag{3.139}$$

3.3 Numerical Results

In this section we discuss how well the amplitude from Lindstedt's method (Equations (3.138) - (3.139)) fits the behavior of the queueing system. We consider the queue lengths to be determined with sufficient accuracy by numerical integration of Equations (3.74) - (3.77) using MATLAB's 'dde23' function, so we will test our approximation against the numerical integration results.

Lindstedt's method is highly accurate when the delay is close to the threshold value. Figures (19) - (20) demonstrate that by comparing the numerically found amplitude and Lindstedt's amplitude as functions of delay for parameters $(\lambda, \mu) = (20, 1)$, where in each figure the approximation is best around $\tau = 0$ (or $\Delta = \Delta_{cr}$). This is expected because Lindstedt's method perturbs the system about its point of bifurcation, so as $\Delta \to \Delta_{cr}$, the predicted amplitude must approach the true amplitude. Once the gap between the delay and Δ_{cr} increases, however, Lindstedt's method cannot provide theoretical guarantees, and in practice the approximation loses accuracy.

More interestingly, the choice of λ and μ affects the accuracy of the fit. Figure (21) shows the surface plot of the absolute error of amplitude for varying λ and Δ, while $\mu = 1$. It is clear that for any delay the approximation is most accurate for the smallest arrival rate λ. A similar observation holds for the service rate μ - for any delay we find the best approximation to be the one corresponding to the largest μ. Figure (22) shows it by recording the absolute error of the approximation for varying values of μ and Δ while $\lambda = 10$.

To summarize, Lindstedt's method performs favorably when the delay is close to Δ_{cr}, when μ is large or λ is small. However, the method's performance decreases once the parameters leave that limited range. Using insight from this method, we propose a different numerical method that maintains accuracy on a larger range of parameters.

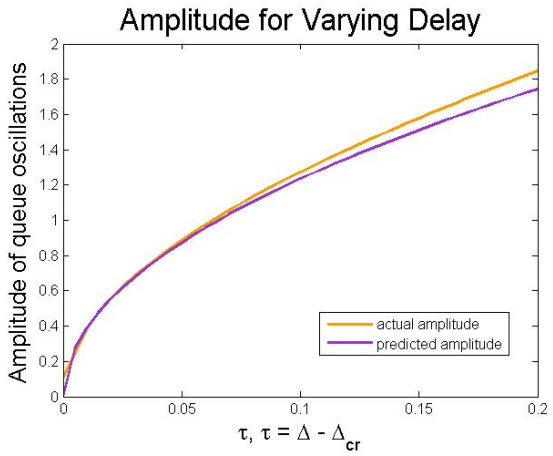

Figure 19: $\lambda = 20$, $\mu = 1$.

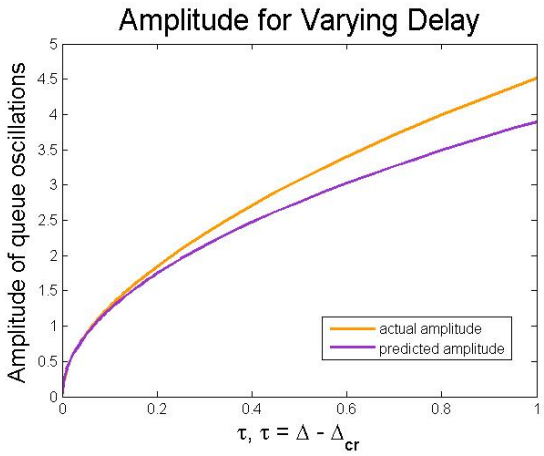

Figure 20: $\lambda = 20$, $\mu = 1$.

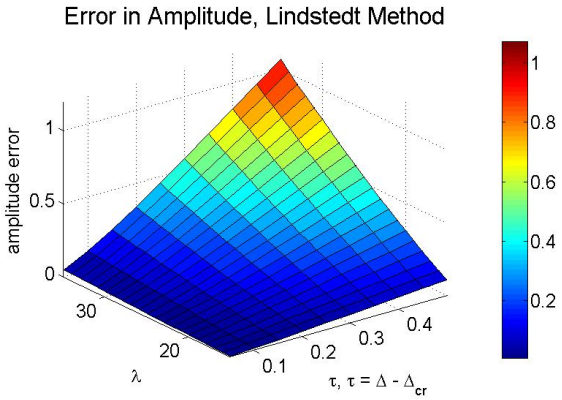

Figure 21: Varying λ.

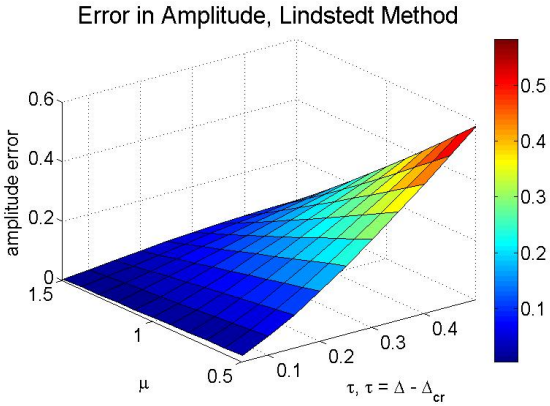

Figure 22: Varying μ.

3.4 Fitting the Slope Function

From general Hopf theory, it is known that the amplitude is usually proportional to the square root of the difference of the delay and the critical delay, and Lindstedt's method confirms that it is true for our model as well. Hence we approximate

$$\text{Amplitude} \approx C(\lambda, \mu) \cdot \sqrt{\Delta - \Delta_{cr}}, \tag{3.140}$$

where $C(\lambda, \mu)$ is a function that depends on the arrival rate λ and the service rate μ. We apply the statistical method to determine $C(\lambda, \mu)$, which we'll refer to as the **slope function**. The goal is to get an approximation for the amplitude that remains accurate over a wider range of parameters than Lindstedt's method allows.

The Algorithm

For a given pair of parameters λ_1 and μ_1 we define $C(\lambda_1, \mu_1)$ to be such that for the predicted amplitude $A_p = C\sqrt{\tau}$, the error $A_p - A$ is minimized in the least squares sense. Here $A(\tau)$ is

the amplitude determined for λ_1 and μ_1 via numerical integration for a finite number points K: $\tau = \Delta - \Delta_{cr} = 0, d, 2d, ..., (K-1)d$. As shown by Equations (2.56) - (2.58), the slope function at (λ_1, μ_1) is given by

$$C = \frac{\sum_{j=0}^{K-1} \sqrt{jd} A(jd)}{\sum_{j=0}^{K-1} jd}. \tag{3.141}$$

Figures (23) and (24) show the slope function's approximation of the amplitude compared to Lindstedt's method for $\lambda = 20$ and $\lambda = 50$, respectively. The slope function is visibly closer to the true value of amplitude than is the approximation from Lindstedt's method.

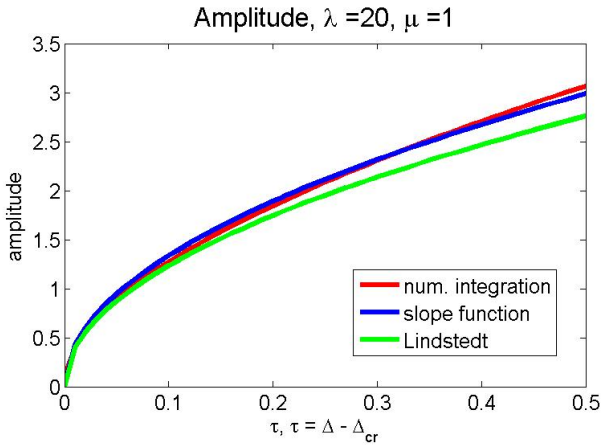

Figure 23: Amplitude prediction comparison.

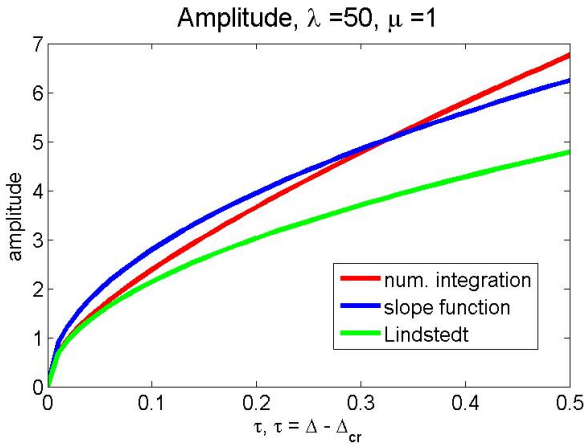

Figure 24: Amplitude prediction comparison.

We extrapolate to find slope function at arbitrary λ and μ based on the function's values computed for a few points. To do so we assume that $C(\lambda, \mu)$ is a separable function

$$C(\lambda, \mu) = \Lambda(\lambda) M(\mu), \tag{3.142}$$

where Λ and M can be approximated by first degree polynomials

$$\Lambda(\lambda) = l_0 + l_1 \lambda \tag{3.143}$$
$$M(\mu) = m_0 + m_1 \mu. \tag{3.144}$$

Our assumption about the form of Λ and M is based on experimental data, which shows that within a sufficient range of (λ, μ) the slope function is very close to linear in λ while μ is kept constant, and it is close to a linear function of μ while λ is constant. This behavior with respect to λ and μ is demonstrated in Figures (25) - (26), respectively, where the blue line in each plot represents the values of $C(\lambda, \mu)$ computed according to Equation (3.141).

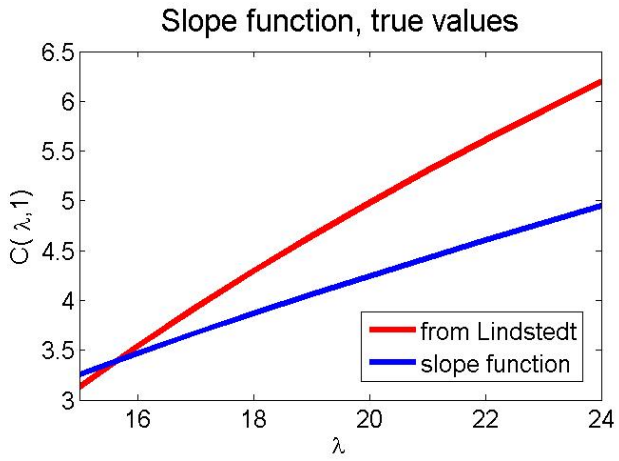

Figure 25: C is approximately linear in λ.

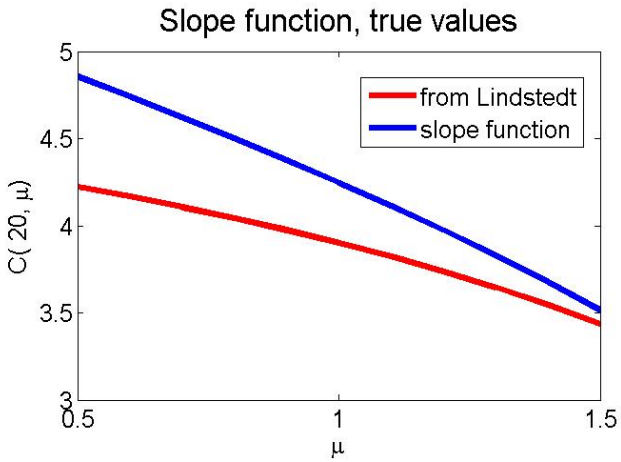

Figure 26: C is approximately linear in μ.

The slope function can be reduced to the form

$$C(\lambda,\mu) = l_1 m_1 (1_{10} + \lambda)(m_{10} + \mu), \qquad l_0 = l_{10} l_1, \qquad m_0 = m_{10} m_1, \tag{3.145}$$

where the unknown coefficients are given by the formulas

$$l_{10} = \frac{\lambda_1 - x_1 \lambda_2}{x_1 - 1}, \qquad x_1 = \frac{C(\lambda_1,\mu_1)}{C(\lambda_2,\mu_1)}, \tag{3.146}$$

$$m_{10} = \frac{\mu_1 - x_2 \mu_2}{x_2 - 1}, \qquad x_2 = \frac{C(\lambda_1,\mu_1)}{C(\lambda_1,\mu_2)}, \tag{3.147}$$

$$l_1 m_1 = \frac{C(\lambda_1,\mu_2)}{(l_{10} + \lambda_1)(m_{10} + \mu_2)}, \tag{3.148}$$

given that slope function at $(\lambda_1,\mu_1), (\lambda_2,\mu_1), (\lambda_1,\mu_2)$ is found by Equation (3.141).
When computed, the values of coefficients l_{10}, m_{10}, and $l_1 m_1$ will slightly vary depending on which parameters λ_1, λ_2, μ_1, and μ_2 are chosen. This happens because the linearity assumption of Λ and M is only an approximation of the true behavior, as shown in Figures (25) - (26). Hence, for optimal results one should choose the data points $C(\lambda_1,\mu_1)$, $C(\lambda_2,\mu_1)$, and $C(\lambda_1,\mu_2)$ around the range of λ and μ that one is interested in.

3.5 Numerical Results for Slope Function

Figures (27) and (28) show the absolute error of amplitude resulting from estimation by the slope function (plot on the left) and by Lindstedt's method (plot on the right) for varying λ and Δ. Overall the slope function results in a smaller error for a wide range of values of λ and Δ, with a maximum error of 0.24 compared to a maximum error of 1.07 in Lindstedt's approximation (that's more than 4 times smaller). However, unlike Lindstedt's technique the slope function doesn't guarantee to be accurate when Δ approaches Δ_{cr}. Hence, it is more advantageous to use the slope function for predicting the amplitude when the delay is

sufficiently greater than the critical value, while Lindstedt's method is preferable when the delay is close to the threshold.

A similar observation holds with respect to μ, when λ is treated as a constant. Surface plots (29) and (30) show that over a range of μ and Δ the slope function has a maximum error of less than a third of Lindstedt's error, being outperformed only when the delay approaches the critical value.

The slope function method is a worthy enhancement of Lindstedt's method that borrows the form derived in Lindstedt's method (the amplitude's proportionality to the square root of difference between total delay and critical delay). The slope function is adaptable, in the sense that it can minimize the error for whichever range of λ, μ, and Δ is required. However, a smaller specified range will yield higher accuracy since functions $\Lambda(\lambda)$ and $M(\mu)$ will have less deviation from linearity over smaller intervals. Lastly, the slope function is computationally more expensive than Lindstedt's method, but still is relatively cheap as it only requires to perform numerical integration of the queueing system at three points (λ, μ) in order to determine the function's value over the range of interest.

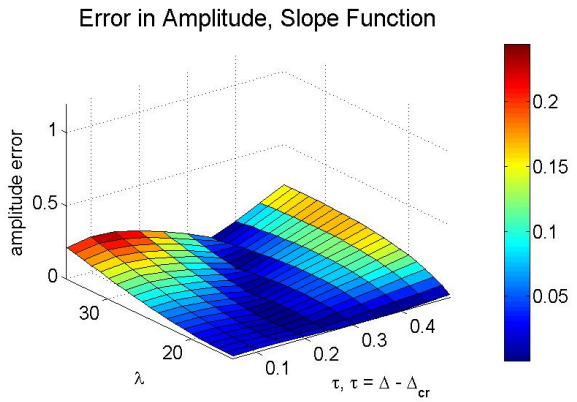

Figure 27: Absolute error from the slope function, with $\mu = 1$.

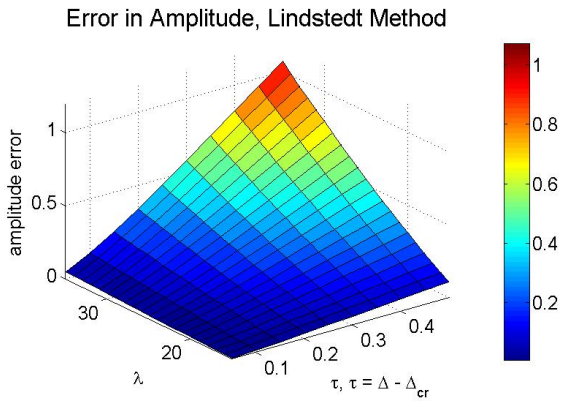

Figure 28: Absolute error from Lindtsedt's method, with $\mu = 1$.

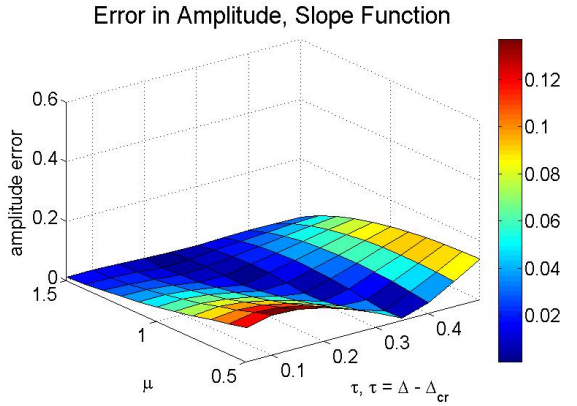

Figure 29: Absolute error from the slope function, with $\lambda = 20$.

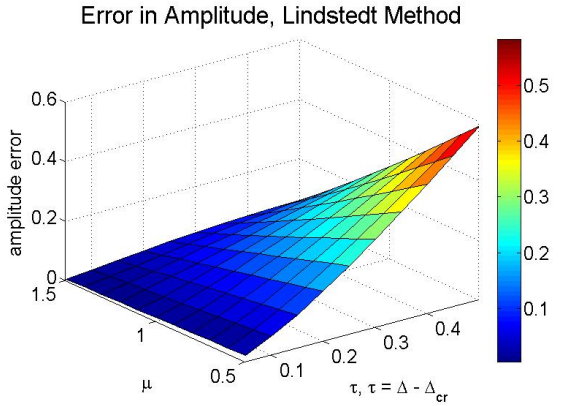

Figure 30: Absolute error from Lindtsedt's method, with $\lambda = 20$.

4 Conclusion

In this paper, we analyze two queueing models that incorporate customer choice and delayed queue length information. The first is a constant delay model and the second is a moving average based model. We analyze the qualitative behavior of the different queueing models and show the occurrence of Hopf bifurcations in both models. Using Lindstedt's method, we construct a new analytic approximation for the amplitude of oscillations that the queueing system exhibits after the Hopf bifurcation. This approximation is computationally much faster than the alternative approach of numerical integration of the system of delay differential equations. We observe that Lindstedt's method works favorably for a certain range of parameters λ, μ, and where Δ is near the critical delay value. Since Lindstedt's method starts to break for larger values of Δ, we develop a new statistical method that estimates how the slope of the amplitude grows as a function of λ and μ. We show that this statistical method maintains a low error across a much wider range of the parameters than Lindsted't method. Although it is more computationally heavy than Lindstedt's method, it is still quite fast to compute and is much cheaper than numerical integration.

Although we have analyzed an important problem, there are still many extensions that are worthy of future study. One potential research direction is to generalize our models for N queues instead of just two. This requires knowledge of tensors and it is not clear that our approach of applying various linear transformations will help because diagonalizing tensors is non-trivial. Another worthwhile extension is to consider rates λ and μ that are not constant but are functions of time, see [16]. These functions shall be motivated by data on customer arrivals and departures. A final extension is to try to derive theoretical error bounds for the numerical methods we have used. This would provide rigorous insight in how well our approximations behave for different parameter settings. We hope to consider these extensions in future work.

References

[1] R. Ibrahim, M. Armony, and A. Bassamboo, "Does the past predict the future? the case of delay announcements in service systems," 2015.

[2] M. Armony and C. Maglaras, "On customer contact centers with a call-back option: Customer decisions, routing rules, and system design," *Operations Research*, vol. 52, no. 2, pp. 271–292, 2004.

[3] P. Guo and P. Zipkin, "Analysis and comparison of queues with different levels of delay information," *Management Science*, vol. 53, no. 6, pp. 962–970, 2007.

[4] R. Hassin, "Information and uncertainty in a queuing system," *Probability in the Engineering and Informational Sciences*, vol. 21, no. 03, pp. 361–380, 2007.

[5] M. Armony, N. Shimkin, and W. Whitt, "The impact of delay announcements in many-server queues with abandonment," *Operations Research*, vol. 57, no. 1, pp. 66–81, 2009.

[6] P. Guo and P. Zipkin, "The impacts of customers'delay-risk sensitivities on a queue with balking," *Probability in the engineering and informational sciences*, vol. 23, no. 03, pp. 409–432, 2009.

[7] O. Jouini, Y. Dallery, and Z. Akşin, "Queueing models for full-flexible multi-class call centers with real-time anticipated delays," *International Journal of Production Economics*, vol. 120, no. 2, pp. 389–399, 2009.

[8] O. Jouini, Z. Aksin, and Y. Dallery, "Call centers with delay information: Models and insights," *Manufacturing & Service Operations Management*, vol. 13, no. 4, pp. 534–548, 2011.

[9] G. Allon and A. Bassamboo, "The impact of delaying the delay announcements," *Operations research*, vol. 59, no. 5, pp. 1198–1210, 2011.

[10] G. Allon, A. Bassamboo, and I. Gurvich, ""we will be right with you": Managing customer expectations with vague promises and cheap talk," *Operations research*, vol. 59, no. 6, pp. 1382–1394, 2011.

[11] W. Whitt, "Improving service by informing customers about anticipated delays," *Management science*, vol. 45, no. 2, pp. 192–207, 1999.

[12] D. Freund, S. Henderson, and D. Shmoys, "Minimizing multimodular functions and allocating capacity in bike-sharing systems," *arXiv preprint arXiv:1611.09304*, 2016.

[13] S. Tao and J. Pender, "A stochastic analysis of bike sharing systems," *arXiv preprint arXiv:1708.08052*, 2017.

[14] Raina, Gaurav, and Wischik, "Buffer sizes for large multiplexers: Tcp queueing theory and instability analysis.," *Next Generation Internet Networks, 2005.*, IEEE, 2005.

[15] J. Pender, R. H. Rand, and E. Wesson, "Queues with choice via delay differential equations," *International Journal of Bifurcation and Chaos*, 27(4) 1730016, 2017.

[16] J. Pender, R. H. Rand, and E. Wesson, "An asymptotic analysis of queues with delayed information and time varying arrival rates," *Nonlinear Dynamics*, 91:2411-2427, 2018.

[17] Y. So and W. Kuhfeld, "Multinomial logit models," *SUGI 20 conference proceedings*, 1995.

[18] J. Hausman and D. McFadden, "Specification tests for the multinomial logit model," *Econometrica, Vol. 52, No. 5*, 1984.

[19] D. McFadden, "Modelling the choice of residential location," Cowles Foundation Discussion Papers 477, Cowles Foundation for Research in Economics, Yale University, 1977.

[20] K. Train, *Discrete Choice Methods with Simulation*. Cambridge University Press, 2009.

[21] B. H. Fralix and I. J. B. F. Adan, "An infinite-server queue influenced by a semi-markovian environment," *Queueing Systems, Volume 61, Issue 1, pp 6584*, 2009.

[22] D. L. Iglehart, "Limiting diffusion approximations for the many server queue and the repairman problem," *Journal of Applied Probability, Vol. 2, Issue 2, pp 429-441*, 1965.

[23] S. Resnick and G. Samorodnitsky, "Activity periods of an infinite server queue and performance of certain heavy tailed fluid queues," *Queueing Systems, Volume 33, Issue 13, pp 4371*, 1999.

[24] B. L.-W. Anatoli Ivanov and H.-O. Walther, "Unstable hyperbolic periodic solutions of differential delay equations," *World Scientific Series in Applicable Analysis: Volume 1, pp. 301-316*, 1992.

[25] X. Xie, "Uniqueness and stability of slowly oscillating periodic solutions of delay equations with bounded nonlinearity," *Journal of Dynamics and Differential Equations, Vol. 3, No. 4*, 1990.

[26] X. Xie, "Uniqueness and stability of slowly oscillating periodic solutions of delay equations with unbounded nonlinearity," *Journal of Differential Equations, 103*, 1993.

[27] X. Xie, "The multiplier equation and its application to s-solutions of a delay equation," *Journal of Differential Equations, 95*, 1992.

[28] S. N. Chow and H. O. Walther, "Characteristic multipliers and stability of symmetric periodic solutions of $\dot{x}(t) = g(x(t-1))$," *Transactions of the American Mathematical Society, Vol. 307, No. 1, pp. 127-142*, 1988.

[29] A. Skubachevskii and H. O. Walther, "On the floquet multipliers of periodic solutions to non-linear functional differential equations," *Journal of Dynamics and Differential Equations, Vol. 18, No. 2*, 2006.

[30] V. L. Jack Hale, *Introduction to Functional Differential Equations*. Springer Science, 1993.

[31] H. Smith, *An Introduction to Delay Differential Equations with Applications to the Life Sciences*. Springer Science, 2011.

[32] S. L. Das and A. Chatterjee, "Multiple scales without center manifold reductions for delay differential equations near hopf bifurcations," *Nonlinear Dynamics, 30: 323335*, 2002.

[33] S. M. S. Mohamed Belhaq, "Fast parametrically excited van der pol oscillator with time delay state feedback," *International Journal of Non-Linear Mechanics 43, pp 124-130*, 2008.

[34] L. Lazarus, M. Davidow, and R. Rand, "Periodically forced delay limit cycle oscillator," *International Journal of Non-Linear Mechanics*, 94:216-222, 2017.

[35] T. Erneux, *Applied Delay Differential Equations*. Springer Science, 2009.

[36] R. Rand, "Differential-delay equations," in *Complex Systems: Fractionality, Time-Delay and Synchronization*, ch. 3, pp. 83–117, Springer: A.C.J. Luo and J-Q Sun, eds., 2011.

5 Appendix

5.1 Constant Delay Model

5.1.1 Showing the existence and uniqueness of equilibrium

Proof of Theorem (2.3). An equilibrium of a dynamical system requires all functions to be constant with respect to time, so the equilibrium must satisfy the condition

$$\dot{q}_i(t) = 0, \tag{5.149}$$

for each $1 \leq i \leq N$. To show that $q_i^*(t) = \frac{\lambda}{N\mu}$ are a steady state solution, it is sufficient to verify that $q_i^*(t) = q_i^*(t-\Delta) = \frac{\lambda}{N\mu}$ satisfy Equation (5.149) for all $t > 0$:

$$\dot{q^*}_i(t) = \lambda \cdot \frac{\exp(-\frac{\lambda}{N\mu})}{\sum_{j=1}^{N} \exp(-\frac{\lambda}{N\mu})} - \mu\frac{\lambda}{N\mu} = \frac{\lambda}{N} - \frac{\lambda}{N} = 0. \tag{5.150}$$

Therefore $q_i^*(t)$ indeed are a steady state solution.

To show uniqueness, we will argue by contradiction. Suppose there is another equilibrium given by $\bar{q}_i(t)$, $1 \leq i \leq N$, and for some i we have $q_i^* \neq \bar{q}_i$. Without loss of generality, let us assume that it is the N'th queue, therefore

$$q_N^* \neq \bar{q}_N. \tag{5.151}$$

Also, without loss of generality let us assume that $q_N^*(t) > \bar{q}_N(t)$ for some t, and since both are constants with respect to time (as is any steady state solution) the following equality arises

$$\bar{q}_N(t) = \frac{\lambda}{N\mu} + \epsilon, \qquad \epsilon > 0. \tag{5.152}$$

Equation (5.149) must hold so

$$0 = \sum_{i=1}^{N} \dot{\bar{q}}_i(t) = \lambda \cdot \frac{\sum_{i=1}^{N} \exp\big(-\bar{q}_i(t-\Delta)\big)}{\sum_{j=1}^{N} \exp(-\bar{q}_j(t-\Delta))} - \mu \sum_{i=1}^{N} \bar{q}_i(t), \tag{5.153}$$

$$\sum_{i=1}^{N} \bar{q}_i(t) = \frac{\lambda}{\mu}. \tag{5.154}$$

Subtracting Equation (5.152) from Equation (5.154) yields

$$\sum_{i=1}^{N-1} \bar{q}_i(t) = \frac{\lambda}{\mu} - \Big(\frac{\lambda}{N\mu} + \epsilon\Big) = \frac{(N-1)\lambda}{\mu N} - \epsilon, \tag{5.155}$$

which means that there exists some index k, $1 \leq k \leq N-1$, such that

$$\bar{q}_k = \frac{\lambda}{\mu N} - \delta, \qquad \delta > 0. \tag{5.156}$$

Since $\dot{\bar{q}}_k = 0$, we can write out $\dot{\bar{q}}_k$ in its explicit form as

$$\lambda \frac{\exp\big(-\bar{q}_k(t-\Delta)\big)}{\sum_{i=1}^{N} \exp\big(-\bar{q}_i(t-\Delta)\big)} - \mu \bar{q}_k(t) = 0, \tag{5.157}$$

$$\sum_{i=1}^{N} \exp\big(-\bar{q}_i(t-\Delta)\big) = \frac{\lambda}{\mu} \cdot \frac{\exp\big(-\frac{\lambda}{N\mu} + \delta\big)}{(\frac{\lambda}{N\mu} - \delta)}. \tag{5.158}$$

The contradiction now becomes clear:

$$\begin{aligned}
\dot{\bar{q}}_N(t) &= \lambda \frac{\exp\big(-\bar{q}_N(t-\Delta)\big)}{\sum_{i=1}^{N} \exp\big(-\bar{q}_i(t-\Delta)\big)} - \mu \bar{q}_N(t) && (5.159)\\
&= \lambda \frac{\exp\big(-\frac{\lambda}{N\mu} - \epsilon\big)}{\frac{\lambda}{\mu} \cdot \frac{\exp(-\frac{\lambda}{N\mu} + \delta)}{(\frac{\lambda}{N\mu} - \delta)}} - \mu\Big(\frac{\lambda}{N\mu} + \epsilon\Big) && (5.160)\\
&= \mu e^{-\epsilon-\delta}\Big(\frac{\lambda}{N\mu} - \delta\Big) - \mu\Big(\frac{\lambda}{N\mu} + \epsilon\Big) && (5.161)\\
&= -\frac{\lambda}{N}\big(1 - e^{-\epsilon-\delta}\big) - \mu\big(\epsilon + \delta e^{-\epsilon-\delta}\big) < 0. && (5.162)
\end{aligned}$$

This shows that Equation (5.149) is not satisfied so $\bar{q}_N(t)$ is not an equilibrium, and therefore the equilibrium must be unique. □

5.1.2 Third Order Taylor Expansion

A third order Talor expansion is used to approximate the deviation of the queues from the equilibrium. This is required both by the Lindstedt's method for determining the amplitude, and by the the slow flow method for determining the stability of the limit cycle.

Proposition 5.1. *Performing a Taylor series expansion for the deviations from the equilibrium state* (2.7) *of equations* (2.2) - (2.3) *and keeping terms up to the third order yields the following system of delay differential equations* $w_1(t)$ *and* $w_2(t)$*:*

$$\dot{w}_1(t) = \lambda\left(-\frac{w_1 - w_2}{4} + \frac{w_1^3 - 3w_2w_1^2 + 3w_1w_2^2 - w_2^3}{48}\right)(t-\Delta) - \mu w_1(t) \tag{5.163}$$

$$\dot{w}_2(t) = \lambda\left(-\frac{w_2 - w_1}{4} + \frac{w_2^3 - 3w_1w_2^2 + 3w_2w_1^2 - w_1^3}{48}\right)(t-\Delta) - \mu w_2(t). \tag{5.164}$$

Proof. We begin with the coupled delay-differential equations (2.2) - (2.3) and we define new functions $\tilde{u}_1$ and $\tilde{u}_2$ that represent the deviation of the queues q_1 and q_2 from the equilibrium state at $\frac{\lambda}{2\mu}$:

$$q_1(t) = \frac{\lambda}{2\mu} + \tilde{u}_1(t) \tag{5.165}$$

$$q_2(t) = \frac{\lambda}{2\mu} + \tilde{u}_2(t). \tag{5.166}$$

The functions $\tilde{u}_1$ and $\tilde{u}_2$ can therefore be described by the differential equations

$$\dot{\tilde{u}}_1(t) = \lambda \cdot \frac{\exp\big(-\tilde{u}_1(t-\Delta)\big)}{\exp\big(-\tilde{u}_1(t-\Delta)\big) + \exp\big(-\tilde{u}_2(t-\Delta)\big)} - \mu\tilde{u}_1(t) - \frac{\lambda}{2} \tag{5.167}$$

$$\dot{\tilde{u}}_2(t) = \lambda \cdot \frac{\exp\big(-\tilde{u}_2(t-\Delta)\big)}{\exp\big(-\tilde{u}_1(t-\Delta)\big) + \exp\big(-\tilde{u}_2(t-\Delta)\big)} - \mu\tilde{u}_2(t) - \frac{\lambda}{2}. \tag{5.168}$$

We approximate $\dot{\tilde{u}}_1(t)$ and $\dot{\tilde{u}}_2(t)$ by a third degree polynomial around the point $\tilde{u}_1(t) = \tilde{u}_2(t) = 0$, which is equivalent to performing Taylor expansion up to the cubic terms. Note that the point $\tilde{u}_1(t) = \tilde{u}_2(t) = 0$ is equivalent to $q_1(t) = q_2(t) = \frac{\lambda}{2\mu}$, which is the equilibrium point. The functions with the approximated derivatives are $w_1(t)$ and $w_2(t)$:

$$\dot{w}_1(t) = \lambda\Big(-\frac{w_1 - w_2}{4} + \frac{w_1^3 - 3w_2w_1^2 + 3w_1w_2^2 - w_2^3}{48}\Big)(t-\Delta) - \mu w_1(t) \tag{5.169}$$

$$\dot{w}_2(t) = \lambda\Big(-\frac{w_2 - w_1}{4} + \frac{w_2^3 - 3w_1w_2^2 + 3w_2w_1^2 - w_1^3}{48}\Big)(t-\Delta) - \mu w_2(t). \tag{5.170}$$

□

5.1.3 Reduction to One Cubic Delay Equation

The symmetry of Equations (5.163) - (5.164) allows the equations to become uncoupled. We consider sum and the difference of w_1 and w_2,

$$\tilde{v}_1(t) = w_1(t) + w_2(t), \quad \tilde{v}_2(t) = w_1(t) - w_2(t). \tag{5.171}$$

This change of variables leads to the differential equations

$$\dot{\tilde{v}}_1(t) = -\mu\big(w_1(t) + w_2(t)\big) = -\mu\tilde{v}_1(t) \tag{5.172}$$

$$\dot{\tilde{v}}_2(t) = \lambda\left(-\frac{\tilde{v}_2(t-\Delta)}{2} + \frac{\tilde{v}_2^3(t-\Delta)}{24}\right) - \mu\tilde{v}_2(t), \tag{5.173}$$

so the two equations become uncoupled. Equation (5.172) has the solution

$$\tilde{v}_1(t) = Ce^{-\mu t} \tag{5.174}$$

so $\tilde{v}_1(t)$ decays to 0 regardless of what the delay parameter is. The oscillations must therefore by represented in the function $\tilde{v}_2(t)$ from Equation (5.173).

5.2 Moving Average Model

5.2.1 Showing the existence and uniqueness of equilibrium

Proof of Theorem (3.1). The proof first shows the existence and uniqueness of the equilibrium

$$q_1^*(t) = q_2^*(t) = m_1^*(t) = m_2^*(t) = \frac{\lambda}{2\mu}, \tag{5.175}$$

and then shows the conditions under which this equilibrium is stable.

Suppose the queues are in equilibrium. Then $q_1(t) = q_1^*$, $q_2(t) = q_2^*$, $m_1(t) = \frac{1}{\Delta}\int_{t-\Delta}^{t} q_1(s)ds = q_1^*$, and $m_2(t) = \frac{1}{\Delta}\int_{t-\Delta}^{t} q_2(s)ds = q_2^*$. By summing Equations (3.74) - (3.75) we find

$$\lambda - \mu(q_1^* + q_2^*) = 0, \quad q_1^* = \frac{\lambda}{\mu} - q_2^*. \tag{5.176}$$

Eliminating q_1^* from Equations (3.74) - (3.75) and subtracting one equation from the other, we find that for $x = 2q_2^* - \frac{\lambda}{\mu}$

$$x = \frac{\lambda}{\mu}\left(\frac{1 - e^x}{1 + e^x}\right). \tag{5.177}$$

Since $\frac{\lambda}{\mu} > 0$, when $x > 0$ the right-hand side of Equation (5.177) is negative so $x \leq 0$. Similarly, when $x < 0$ then the right hand side of the equation is positive, which means that $x = 0$ is the only solution. Hence $q_2^* = \frac{\lambda}{2\mu}$ and $q_1^* = \frac{\lambda}{\mu} - q_2^* = \frac{\lambda}{2\mu}$ is the only equilibrium point of $q_1(t)$ and $q_2(t)$, which implies that $m_1(t) = m_2(t) = \frac{\lambda}{2\mu}$.

This equilibrium is stable by the choice of Δ_{cr}. We will show that for the specified range of Δ, all eigenvalues of the characteristic equation (3.83) have negative real parts. Proposition (3.5) shows that any nontrivial real eigenvalue must be negative. A trivial eigenvalue $\Lambda = 0$ implies that the queues are constant, in which case the equilibrium is obviously stable. Hence, it remains to show that the complex eigenvalues have negative real parts.

Case 1. Suppose the characteristic equation (3.86) does not have positive roots Δ_{cr}. This implies that a complex eigenvalue Λ never reaches the imaginary axis as Δ varies. Since Λ is continuous as a function of Δ, then $\mathrm{Re}[\Lambda]$ must be of the same sign for all $\Delta > 0$. Proposition (3.7) shows that for sufficiently small Δ, all complex eigenvalues have negative real parts, which therefore is true for all $\Delta > 0$.

Case 2. Suppose Equation (3.86) has at least one positive root Δ_{cr}. By the continuity of Λ with respect to Δ, $\mathrm{Re}[\Lambda]$ must be of the same sign on the interval where Δ is less than the smallest positive root of Equation (3.86), and then Proposition (3.7) shows that $\mathrm{Re}[\Lambda] < 0$. Same holds when $\Delta > \Delta^*$, with Δ^* defined as the largest root of Equation (3.86). Note that $\Delta^* < \frac{\lambda}{\mu^2}$ by Proposition (3.4). Therefore, the continuity of Λ together with Proposition (3.6) means that $\mathrm{Re}[\Lambda] < 0$ when $\Delta > \Delta^*$.

We showed that for the specified ranges of Δ, all eigenvalues have negative real parts and therefore the equilibrium of Equation (5.175) is stable.

□

5.3 Third Order Polynomial Expansion

We will perform a Taylor series expansion for the deviations about the equilibrium (3.87) of equations (3.74) - (3.77) and keep terms up to the third order. To start, we find the perturbations of our functions from the equilibrium,

$$q_1(t) = \tfrac{\lambda}{2\mu} + \tilde{u}_1(t) \tag{5.178}$$

$$q_2(t) = \tfrac{\lambda}{2\mu} + \tilde{u}_2(t) \tag{5.179}$$

$$m_1(t) = \tfrac{\lambda}{2\mu} + \tilde{u}_3(t) \tag{5.180}$$

$$m_2(t) = \tfrac{\lambda}{2\mu} + \tilde{u}_4(t), \tag{5.181}$$

and from Equations (3.74) - (3.77) we find their derivatives:

$$\dot{\tilde{u}}_1(t) = \lambda \cdot \frac{\exp\big(-\tilde{u}_3(t)\big)}{\exp\big(-\tilde{u}_3(t)\big) + \exp\big(-\tilde{u}_4(t)\big)} - \frac{\lambda}{2} - \mu\tilde{u}_1(t) \tag{5.182}$$

$$\dot{\tilde{u}}_2(t) = \lambda \cdot \frac{\exp\big(-\tilde{u}_4(t)\big)}{\exp\big(-\tilde{u}_3(t)\big) + \exp\big(-\tilde{u}_4(t)\big)} - \frac{\lambda}{2} - \mu\tilde{u}_2(t) \tag{5.183}$$

$$\dot{\tilde{u}}_3(t) = \frac{1}{\Delta} \cdot \Big(\tilde{u}_1(t) - \tilde{u}_1(t-\Delta)\Big) \tag{5.184}$$

$$\dot{\tilde{u}}_4(t) = \frac{1}{\Delta} \cdot \Big(\tilde{u}_2(t) - \tilde{u}_2(t-\Delta)\Big). \tag{5.185}$$

A third order Taylor expansion of the terms on the right gives us the functions

$$\begin{aligned}\dot{w}_1(t) &= \lambda \cdot \left(-\frac{w_3(t) - w_4(t)}{4}\right) - \mu w_1(t) \\ &+ \lambda \cdot \left(\frac{w_3^3(t) - 3w_4(t)w_3^2(t) + 3w_3(t)w_4^2(t) - w_4^3(t)}{48}\right)\end{aligned} \tag{5.186}$$

$$\begin{aligned}\dot{w}_2(t) &= \lambda \cdot \left(-\frac{w_4(t) - w_3(t)}{4}\right) - \mu w_2(t) \\ &+ \lambda \cdot \left(\frac{w_4^3(t) - 3w_3(t)w_4^2(t) + 3w_4(t)w_3^2(t) - w_3^3(t)}{48}\right)\end{aligned} \tag{5.187}$$

$$\dot{w}_3(t) = \frac{1}{\Delta}\Big(w_1(t) - w_1(t-\Delta)\Big) \tag{5.188}$$

$$\dot{w}_4(t) = \frac{1}{\Delta}\Big(w_2(t) - w_2(t-\Delta)\Big). \tag{5.189}$$

5.4 Reduction to Two Cubic Delay Equations

We will utilize the symmetry of the equations (5.186) - (5.189) to simplify our problem by uncoupling the four equations. Hence we introduce a change of variables

$$\tilde{v}_1 = w_1 + w_2, \quad \tilde{v}_2 = w_1 - w_2, \quad \tilde{v}_3 = w_3 + w_4, \quad \tilde{v}_4 = w_3 - w_4. \tag{5.190}$$

The time derivatives for the new variables simplify our problem

$$\dot{\tilde{v}}_1 = -\mu\tilde{v}_1(t) \tag{5.191}$$

$$\overset{\bullet}{\tilde{v}}_2 = \lambda\Big(- \frac{\tilde{v}_4(t)}{2} + \frac{\tilde{v}_4(t)^3}{24}\Big) - \mu\tilde{v}_2(t) \tag{5.192}$$

$$\overset{\bullet}{\tilde{v}}_3 = \frac{1}{\Delta}\Big(\tilde{v}_1(t) - \tilde{v}_1(t-\Delta)\Big) \tag{5.193}$$

$$\overset{\bullet}{\tilde{v}}_4 = \frac{1}{\Delta}\Big(\tilde{v}_2(t) - \tilde{v}_2(t-\Delta)\Big) \tag{5.194}$$

because now the variables $\tilde{v}_1$ and $\tilde{v}_3$ are uncoupled from variables $\tilde{v}_2$ and $\tilde{v}_4$ so we only need to work with systems of two differential equations. Furthermore, $\tilde{v}_1(t)$ and $\tilde{v}_3(t)$ can be solved directly and they converge to zero as $t \to \infty$. Hence we are left with only two functions of further interest: $\tilde{v}_2$ and $\tilde{v}_4$.